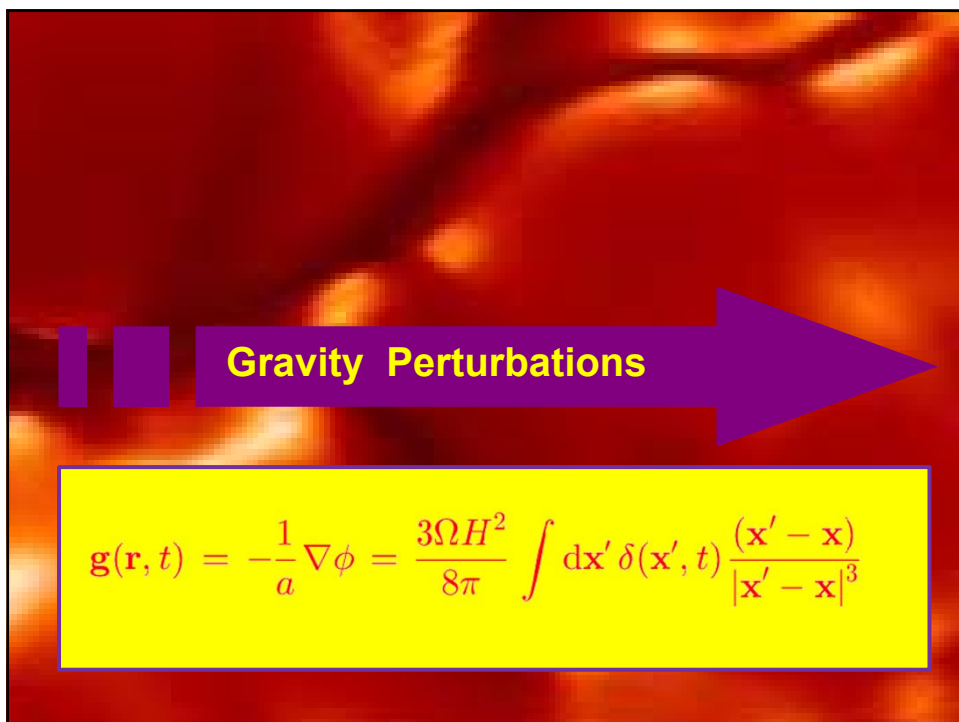
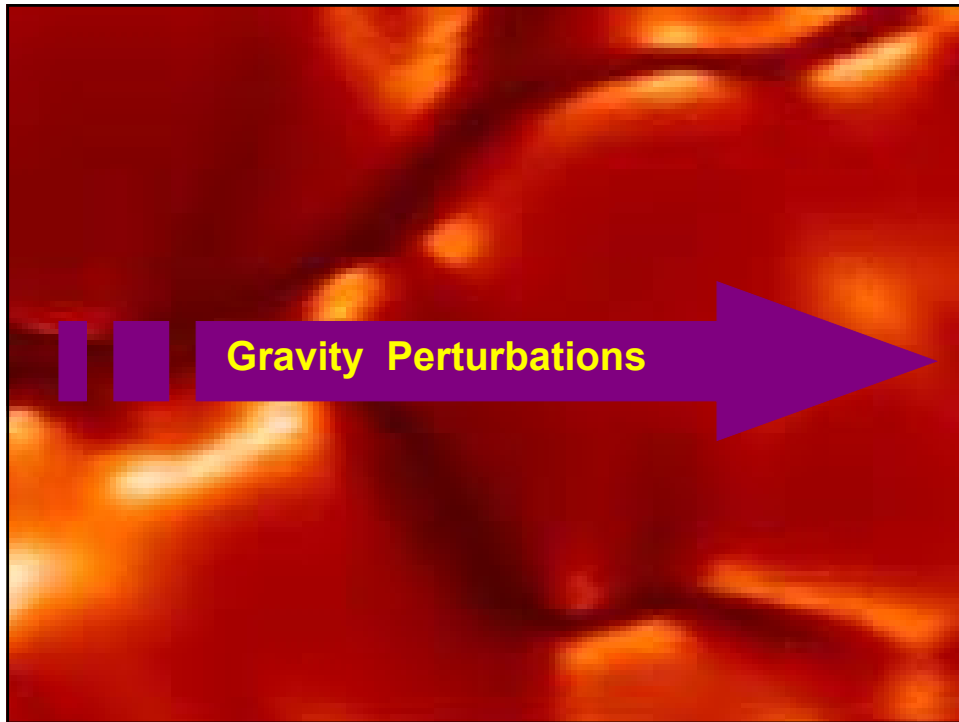
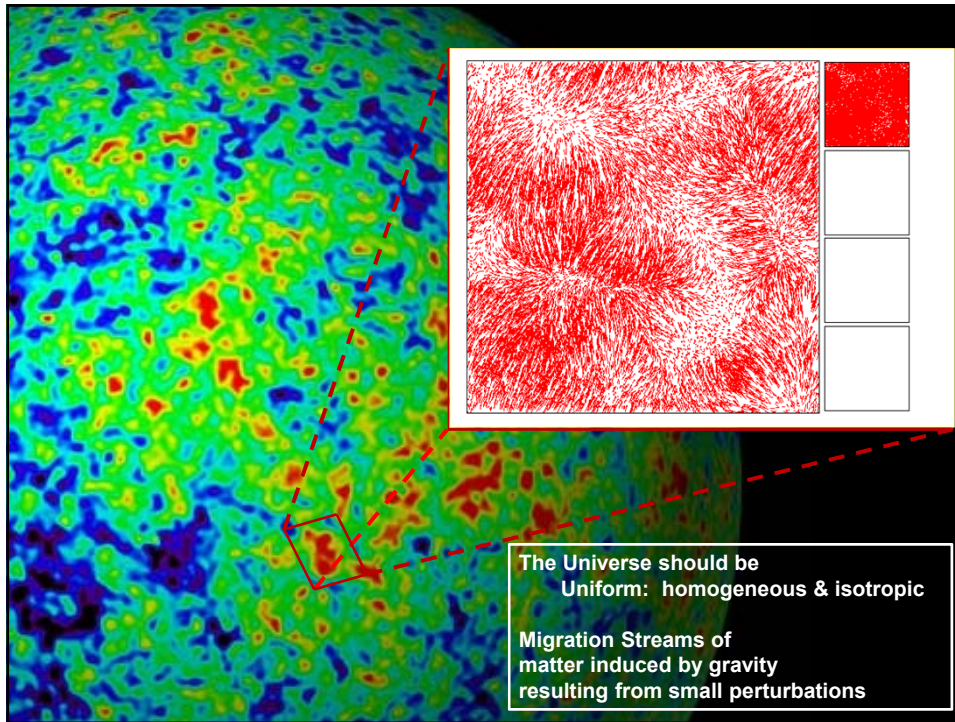


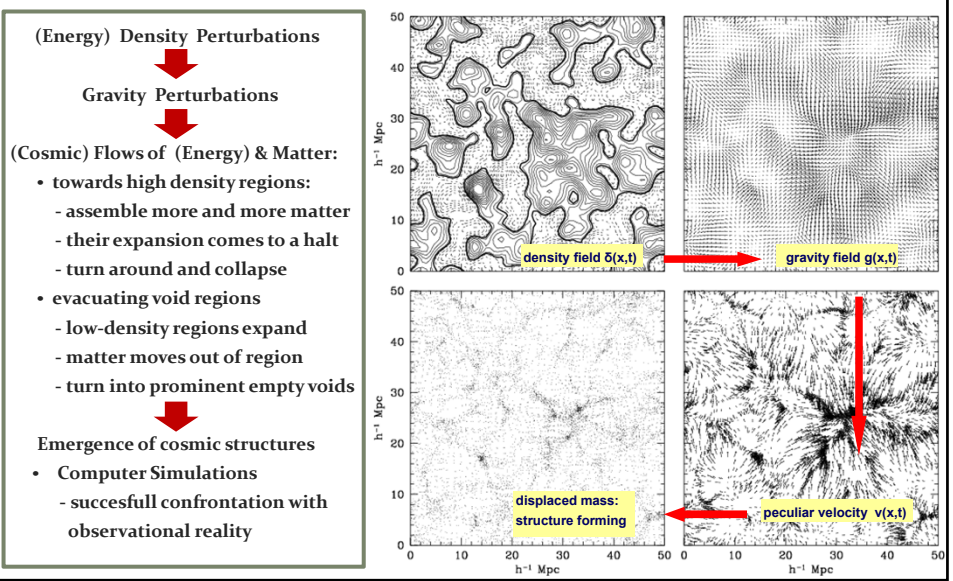
Density Perturbation Field:

$$\delta(\vec{x}, t) = \frac{\rho(x, t) - \rho_u(t)}{\rho_u(t)}$$





Cosmic Structure Formation



Cosmic Structure Formation

Formation
Cosmic Web:

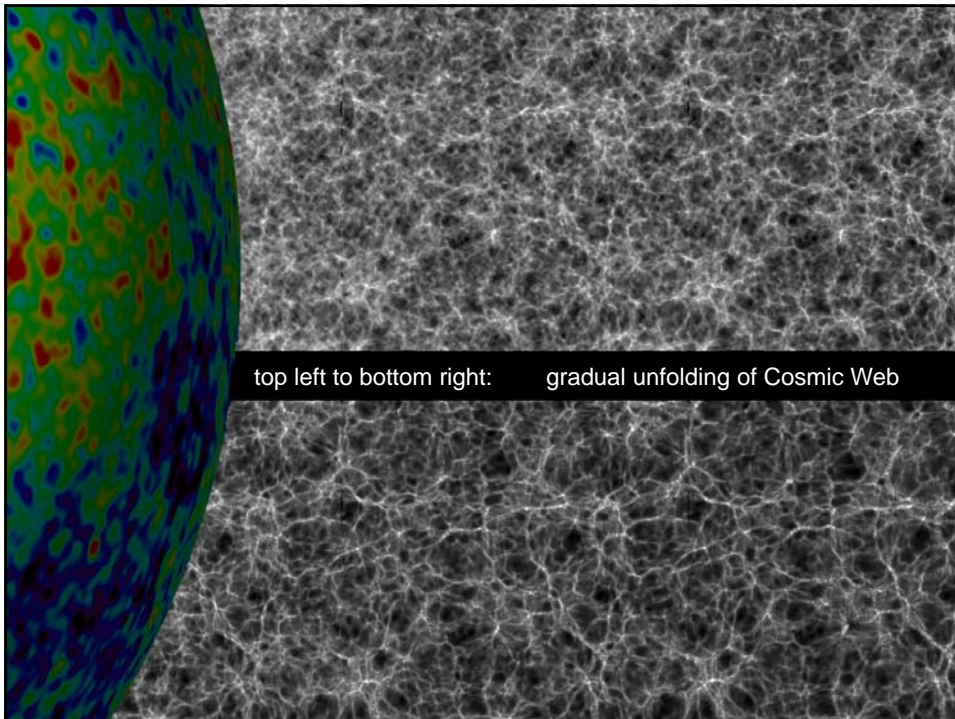
simulation
sequence

(cold)
dark matter

(courtesy:
Virgo/V. Springel).

$z = 20.0$

50 Mpc/h

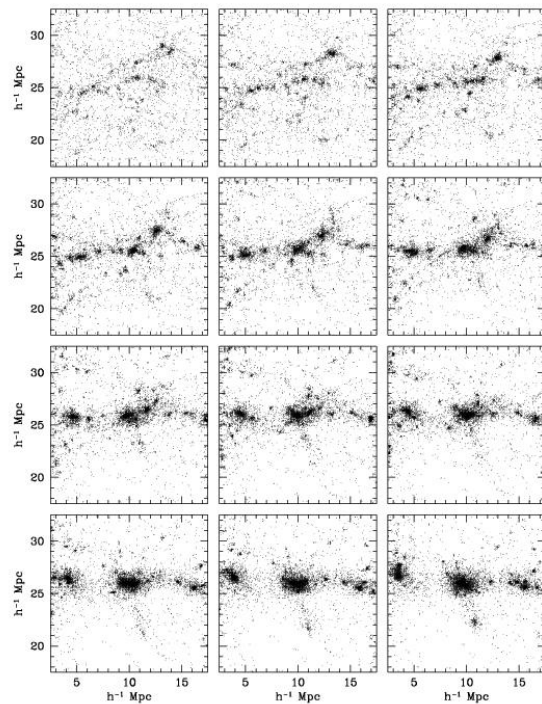


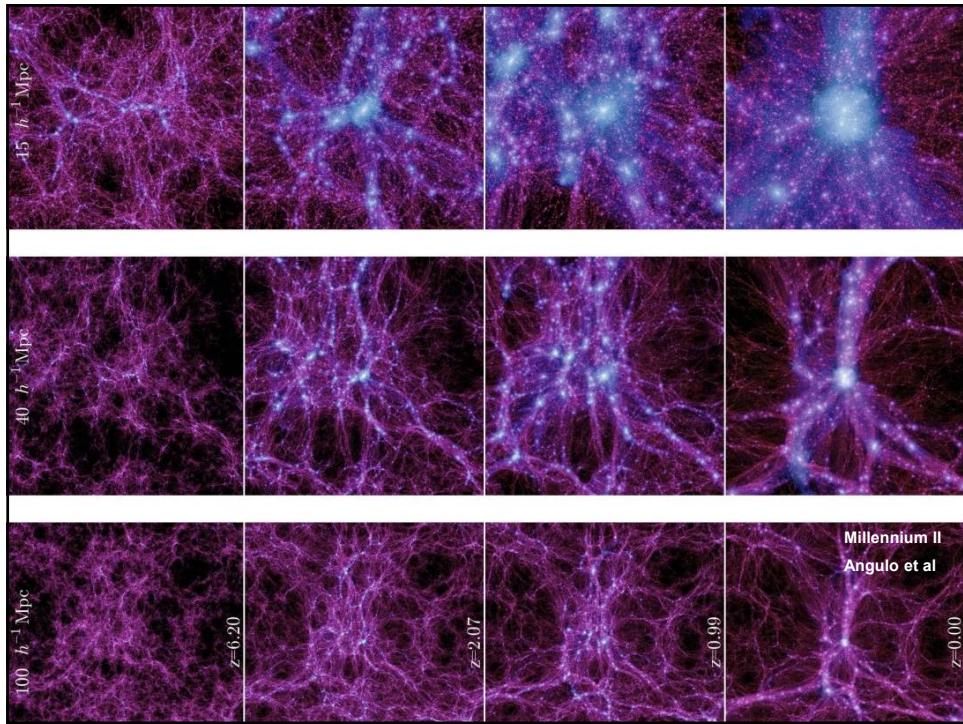
Dynamical Evolution Cosmic Web

- hierarchical structure formation
- anisotropic collapse
- void formation:
asymmetry
overdense vs. underdense

Structures in the Universe form
by
gradual hierarchical assembly:

- ❖ small objects emerge & collapse first,
- ❖ then merge with other clumps
- ❖ while forming larger objects in hierarchy





Voids: Formation & Structure

Void Formation

Void Evolution

an illustration

cosmology:

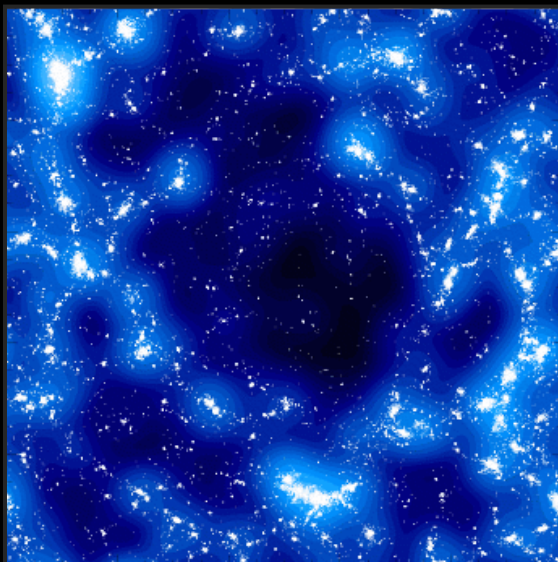
$$\Omega_m = 1.0; \quad H_0 = 70 \text{ km/s/Mpc}$$

initial conditions:

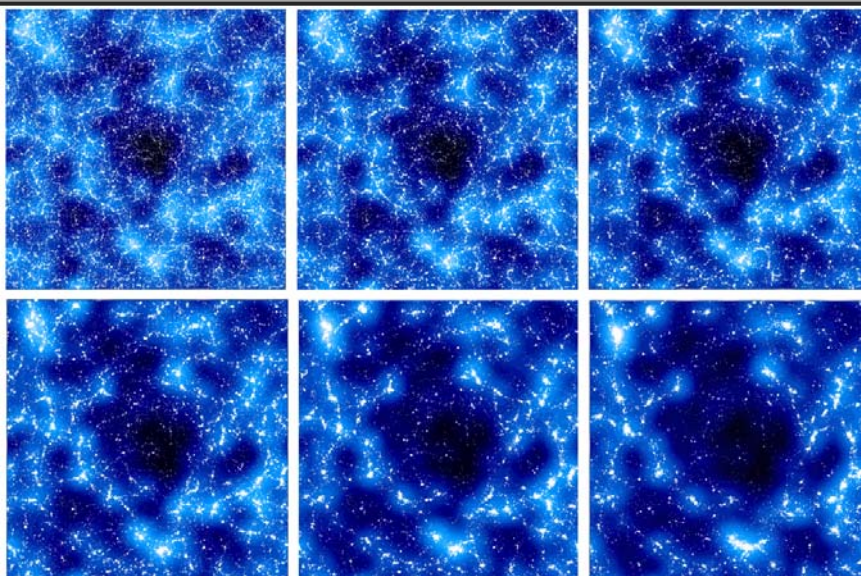
underdensity, Gaussian field

$$R_G \sim 4h^{-1} \text{ Mpc}$$

$$P(k) \propto k^{-0.5}$$



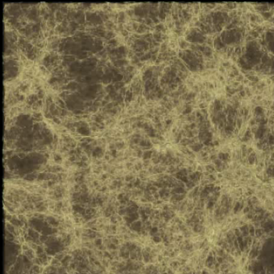
Void Formation



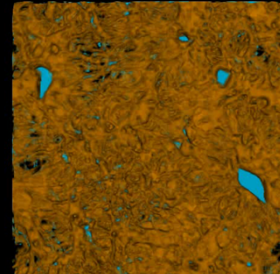
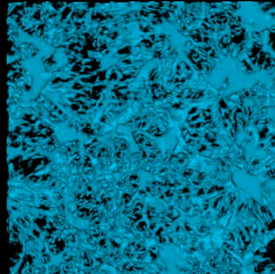
Multiscale Cosmic Web: hierarchical evolution

NEXUS/MMF Evolution Cosmic Web

t = 0.56 Gyrs

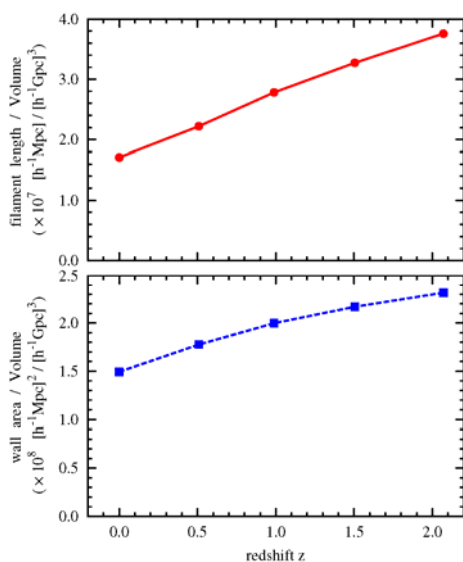


z = 8.70



Cautun et al. 2013

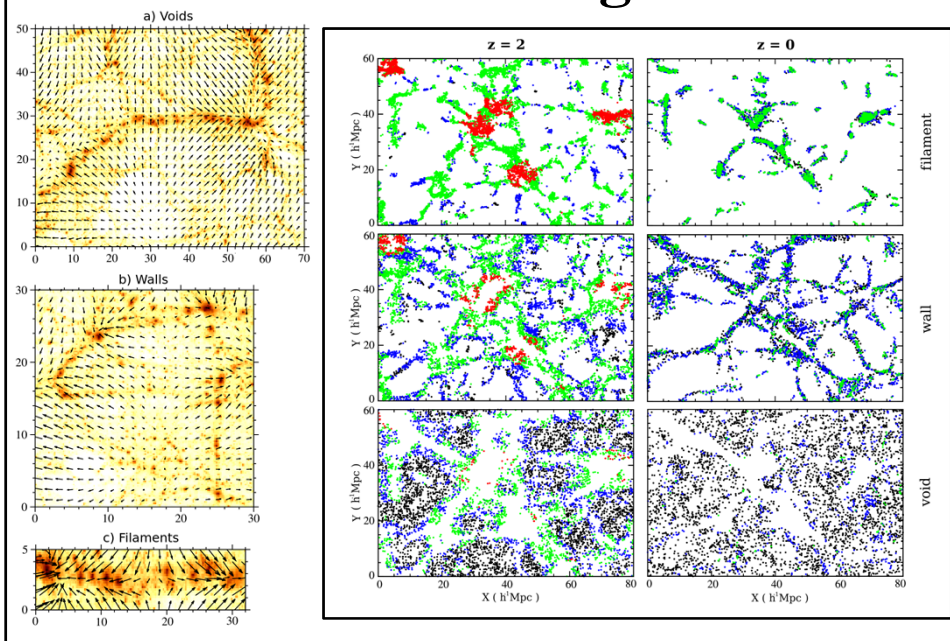
Evolving Filament & Wall Network



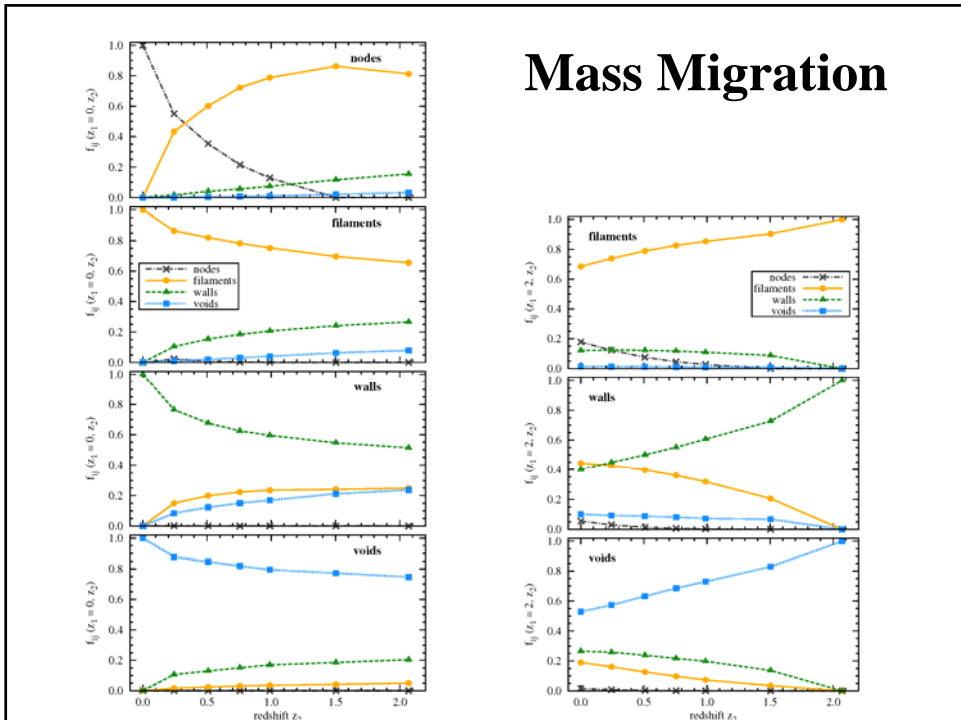
Total length of filament network :
decreasing as a function of time

Total surface area of wall network :
decreasing as a function of time

Web Mass Emigration



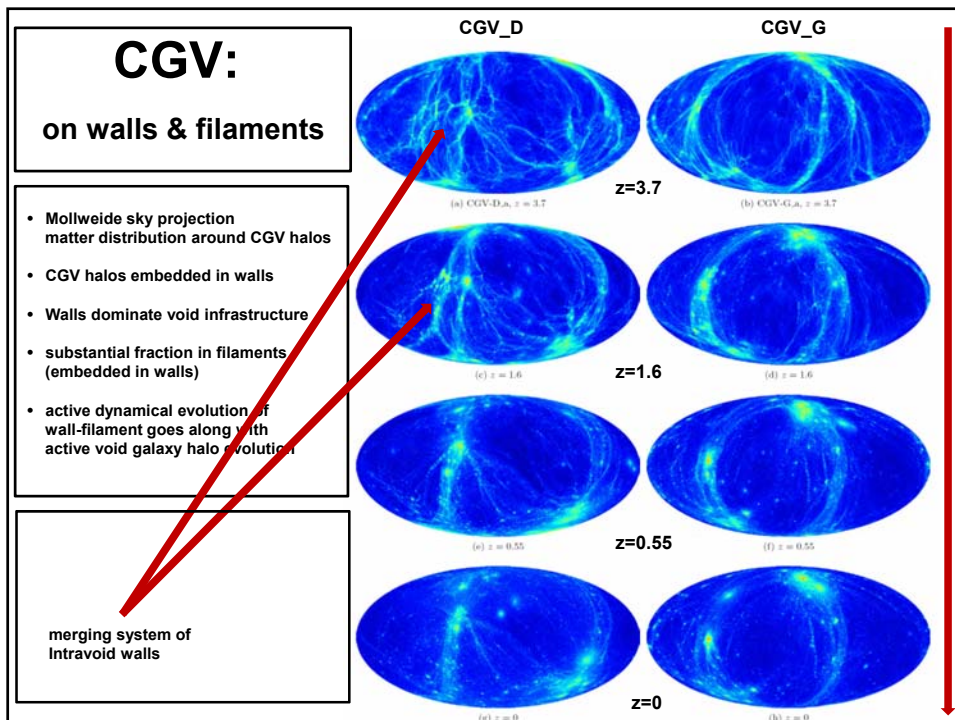
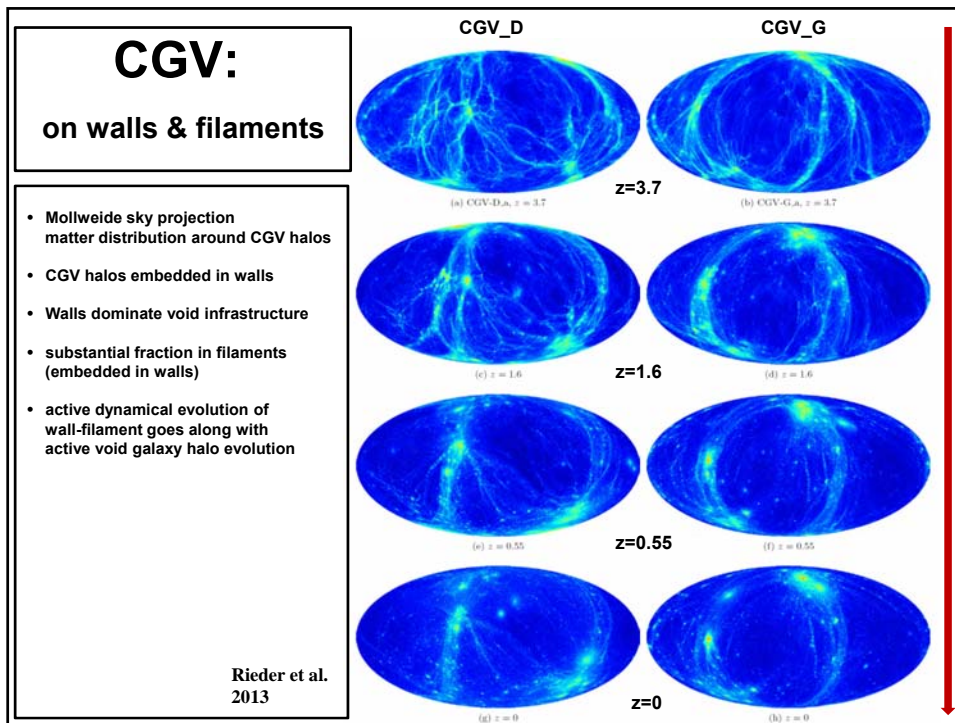
Mass Migration



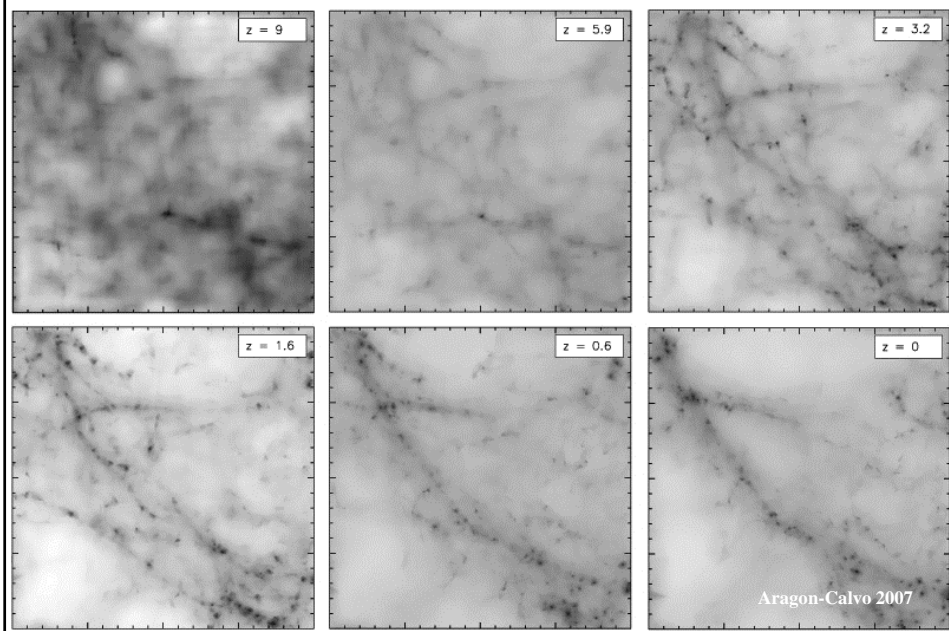
CGV halo & web evolution



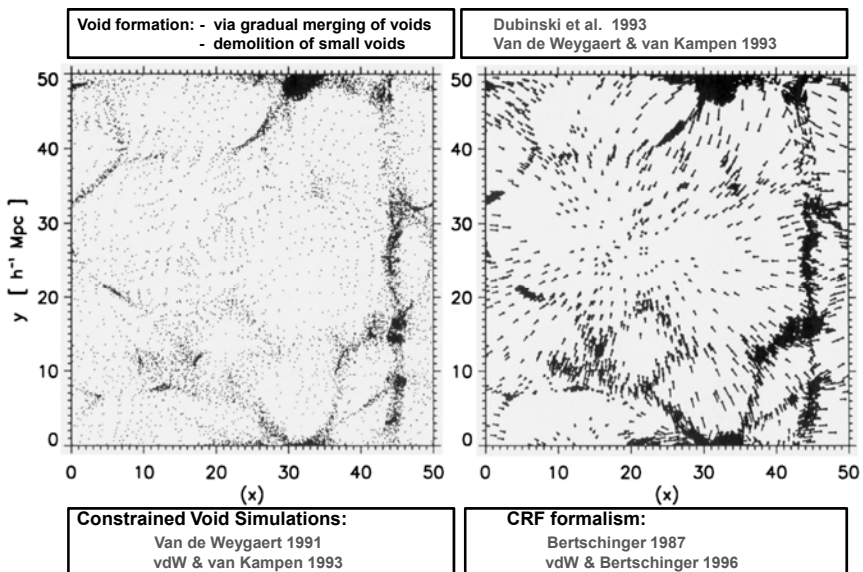
Rieder et al. 2013

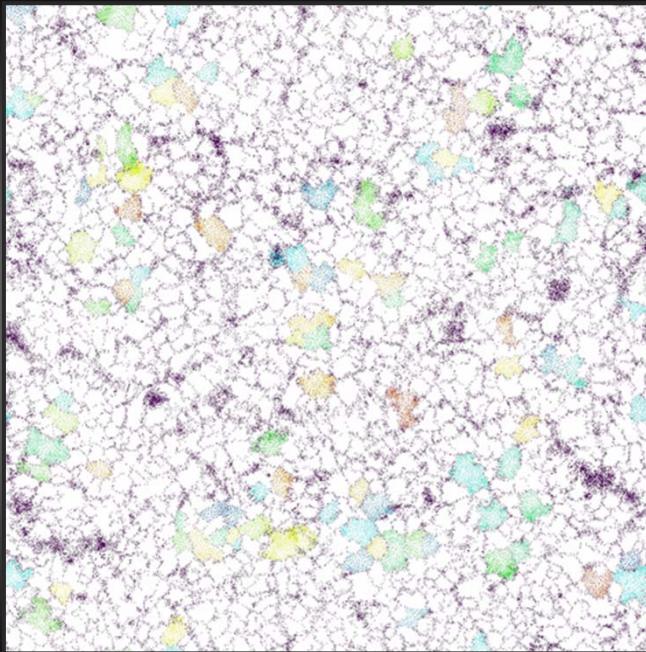


Hierarchical Filament Formation



Void Hierarchy

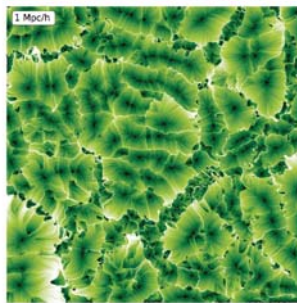
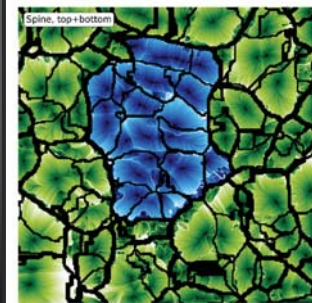
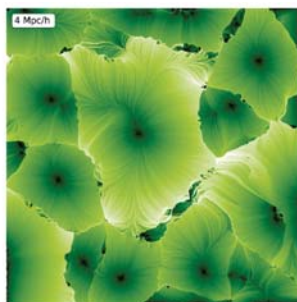
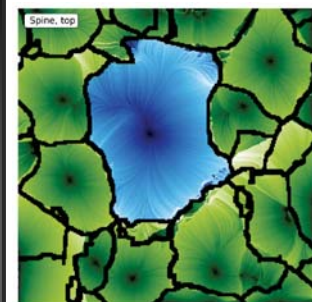




**Hierarchical
Web Evolution:**

“Lagrangian” view:
development and fate
patterns LSS

Platen & vdW 2004



**Hierarchical
Web Evolution:**

Void hierarchy
expressed in
multiscale structure
velocity outflow

Aragon-Calvo & Szalay 2012

Nonlinear Structure Formation

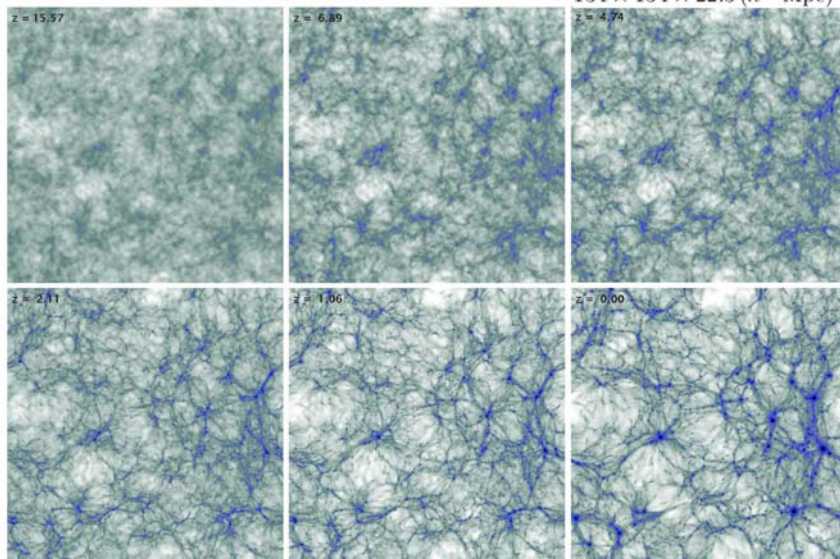
Nbody Simulations

largely based on excellent Potsdam lectures on Nbody simulations (2006)
by V. Springel

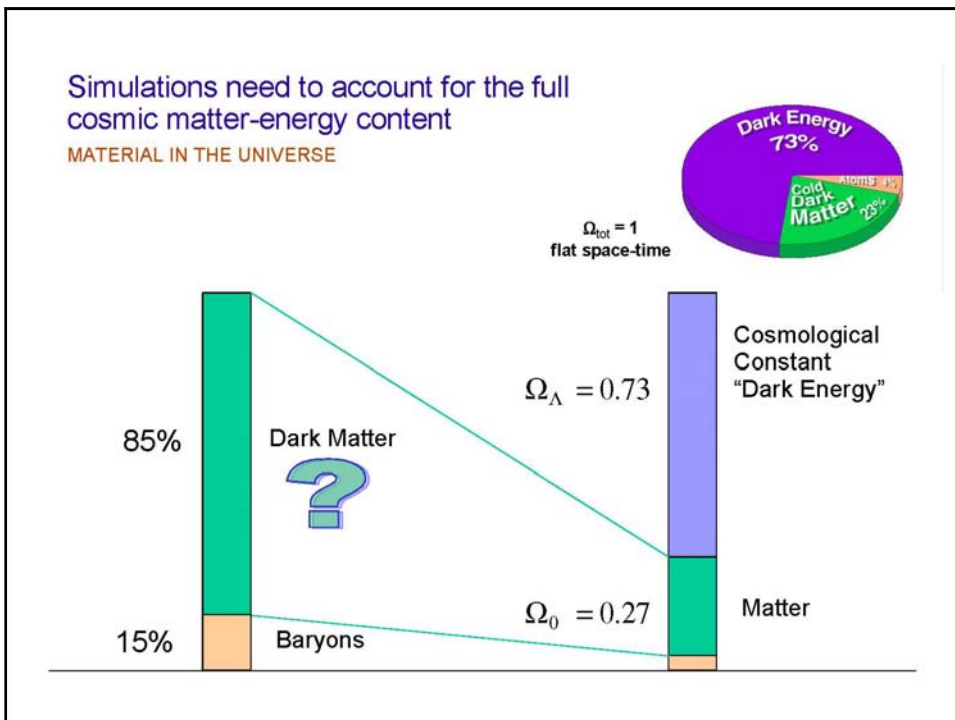
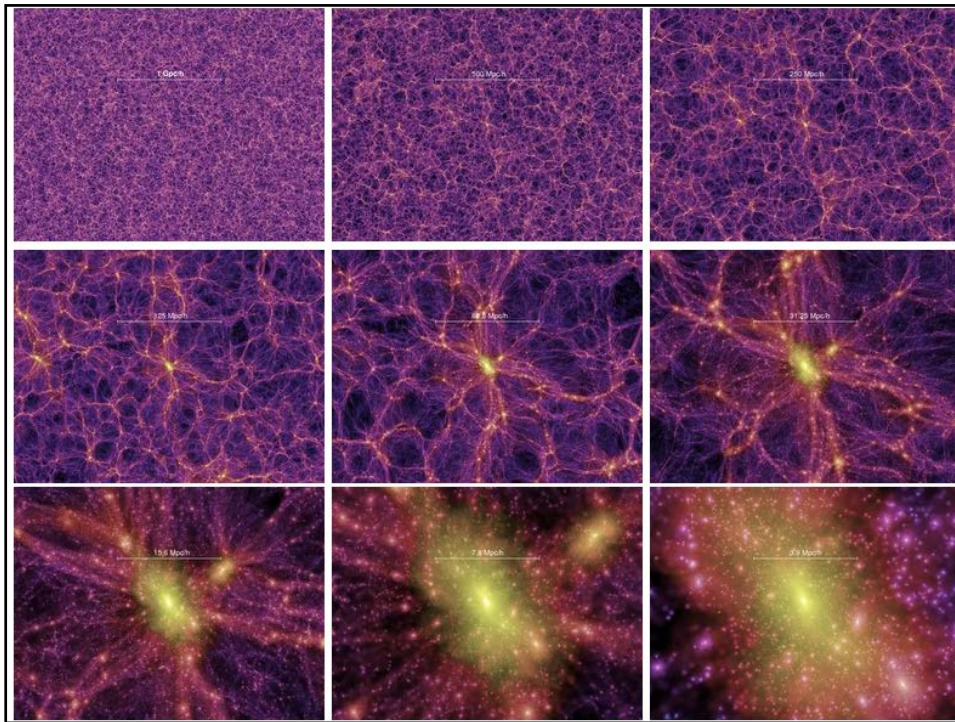
Simulations on scales of order 100 Mpc are the workhorses of
studies of large-scale structure formation

EVOLUTION OF STRUCTURE IN THE GAS DISTRIBUTION

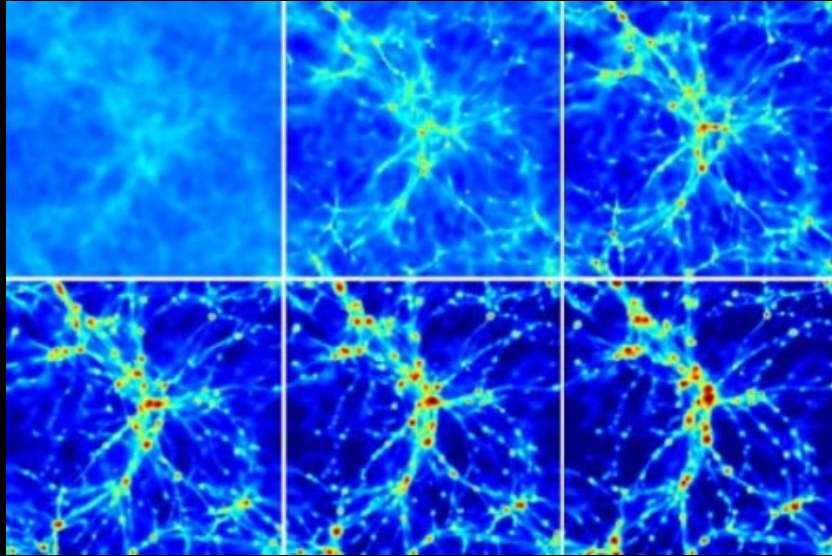
Λ CDM, $N = 2 \times 224^3$
 $134 \times 134 \times 22.3 (h^{-1}\text{Mpc})^3$



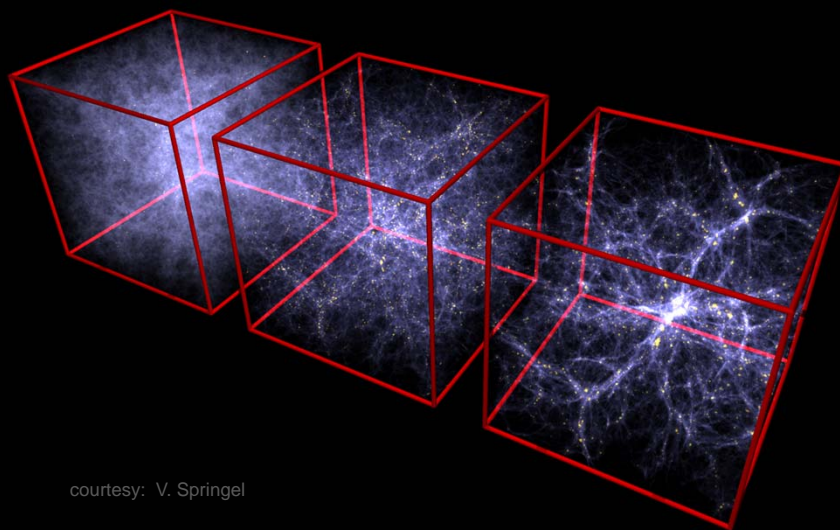
Springel, Hernquist & White (2000)



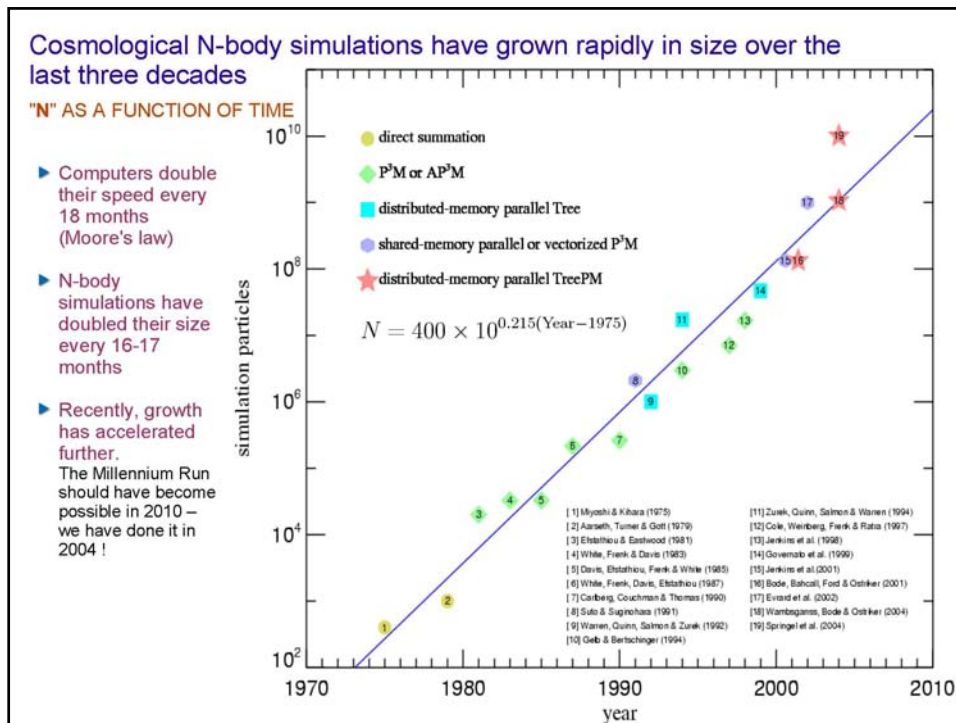
Cosmic Web: Gas Simulation



Gaseous Cosmic Web



courtesy: V. Springel



Nbody Dynamics: Fundamentals

We assume that the only appreciable interaction of dark matter particles is **gravity**

COLLISIONLESS DYNAMICS

Because there are so many dark matter particles, it's best to describe the system in terms of the **single particle distribution function**

$$f = f(\mathbf{x}, \mathbf{v}, t)$$

There are so many dark matter particles that they do not scatter locally on each other, they just respond to their collective gravitational field

Collisionless Boltzmann equation

Poisson-Vlasov System

$$\frac{df}{dt} = \frac{\partial f}{\partial t} + \frac{\partial f}{\partial \mathbf{x}} \cdot \mathbf{v} + \frac{\partial f}{\partial \mathbf{v}} \cdot \left(-\frac{\partial \Phi}{\partial \mathbf{x}} \right) = 0$$

$$\nabla^2 \Phi(\mathbf{x}, t) = 4\pi G \int f(\mathbf{x}, \mathbf{v}, t) d\mathbf{v}$$

Phase-space is conserved along each characteristic (i.e. particle orbit).

The number of stars in galaxies is so large that the two-body relaxation time by far exceeds the Hubble time. Stars in galaxies are therefore also described by the above system.

This system of partial differential equations is very difficult (impossible) to solve directly in non-trivial cases.

The N-body method uses a finite set of particles to sample the underlying distribution function

"MONTE-CARLO" APPROACH TO COLLISIONLESS DYNAMICS

We discretize in terms of N particles, which approximately move along characteristics of the underlying system.

$$\ddot{\mathbf{x}}_i = -\nabla_i \Phi(\mathbf{x}_i)$$

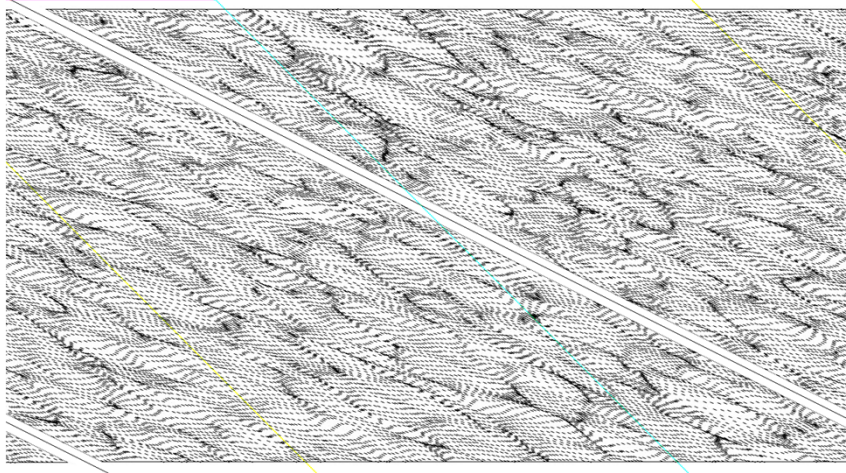
$$\Phi(\mathbf{x}) = -G \sum_{j=1}^N \frac{m_j}{[(\mathbf{x} - \mathbf{x}_j)^2 + \epsilon^2]}$$

The need for **gravitational softening**:

- Prevent large-angle particle scatterings and the formation of bound particle pairs.
- Ensure that the two-body relaxation time is sufficiently large.
- Allows the system to be integrated with low-order intergations schemes.

} Needed for faithful collisionless behaviour

Particle Simulation



Courtesy: J. Hidding

Mass Element Evolution

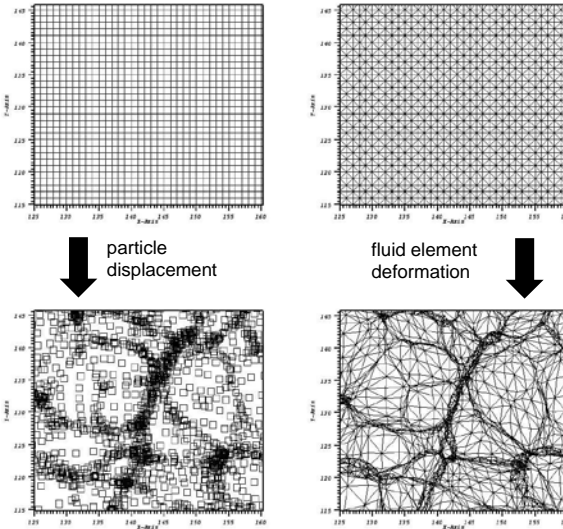


Courtesy: J. Hidding

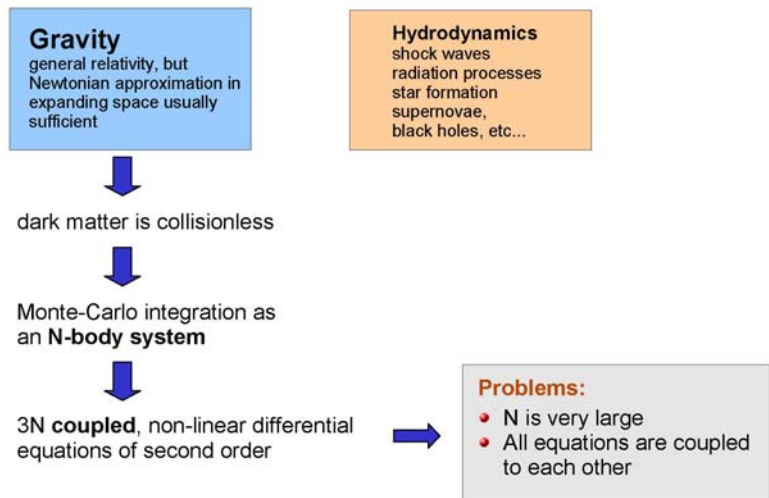
Tessellation Deformation & Phase Space Projection

Translation towards Multi-D space:

- Look at deformation of initial tessellation
- each tessellation cell represents matter cell
- evolution deforms cell
- once cells start to overlap, manifestation of different phase-space matter streams



The dynamics of structure formation is driven by gravity



Two conflicting requirements complicate the study of hierarchical structure formation

DYNAMIC RANGE PROBLEM FACED BY COSMOLOGICAL SIMULATIONS

Want **small particle mass** to resolve internal structure of halos

Want **large volume** to obtain representative sample of universe



need large **N**
where *N* is the particle number

Problems due to a small box size:

- Fundamental mode goes non-linear soon after the first halos form. \Rightarrow Simulation cannot be meaningfully continued beyond this point.
- No rare objects (the first halo, rich galaxy clusters, etc.)

Problems due to a large particle mass:

- Physics cannot be resolved.
- Small galaxies are missed.

At any given time, halos exist on a large range of mass-scales !

Several questions come up when we try to use the N-body approach for cosmological simulations

- How do we compute the gravitational forces efficiently and accurately?
- How do we integrate the orbital equations in time?
- How do we generate appropriate initial conditions?

$$\ddot{\mathbf{x}}_i = -\nabla_i \Phi(\mathbf{x}_i)$$

$$\Phi(\mathbf{x}) = -G \sum_{j=1}^N \frac{m_j}{[(\mathbf{x} - \mathbf{x}_j)^2 + \epsilon^2]}$$

Note: The naïve computation of the forces is an N^2 -task.

Time Integration Issues

Time integration methods

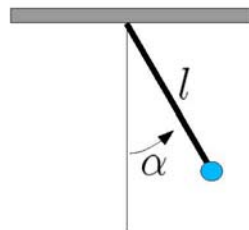
Want to numerically integrate an **ordinary differential equation** (ODE)

$$\dot{\mathbf{y}} = f(\mathbf{y})$$

Note: \mathbf{y} can be a vector

Example: Simple pendulum

$$\ddot{\alpha} = -\frac{g}{l} \sin \alpha$$



$$\begin{aligned} y_0 &\equiv \alpha & y_1 &\equiv \dot{\alpha} \\ \rightarrow \dot{\mathbf{y}} = f(\mathbf{y}) &= \begin{pmatrix} y_1 \\ -\frac{g}{l} \sin y_0 \end{pmatrix} \end{aligned}$$

A numerical approximation to the ODE is a set of values $\{y_0, y_1, y_2, \dots\}$ at times $\{t_0, t_1, t_2, \dots\}$

There are many different ways for obtaining this.

Explicit Euler method

$$y_{n+1} = y_n + f(y_n)\Delta t$$

- Simplest of all
- Right hand-side depends only on things already non, **explicit method**
- The error in a single step is $O(\Delta t^2)$, but for the N steps needed for a finite time interval, the total error scales as $O(\Delta t)$!
- Never use this method, it's only **first order accurate**.

Implicit Euler method

$$y_{n+1} = y_n + f(y_{n+1})\Delta t$$

- **Excellent** stability properties
- Suitable for very stiff ODE
- Requires implicit solver for y_{n+1}

Implicit mid-point rule

$$y_{n+1} = y_n + f\left(\frac{y_n + y_{n+1}}{2}\right)\Delta t$$

- **2nd order accurate**
- Time-symmetric, in fact **symplectic**
- But still implicit...

Runge-Kutta methods

whole class of integration methods

2nd order accurate

$$\begin{aligned} k_1 &= f(y_n) \\ k_2 &= f(y_n + k_1\Delta t) \\ y_{n+1} &= y_n + \left(\frac{k_1 + k_2}{2}\right)\Delta t \end{aligned}$$

4th order accurate.

$$\begin{aligned} k_1 &= f(y_n, t_n) \\ k_2 &= f(y_n + k_1\Delta t/2, t_n + \Delta t/2) \\ k_3 &= f(y_n + k_2\Delta t/2, t_n + \Delta t/2) \\ k_4 &= f(y_n + k_3\Delta t/2, t_n + \Delta t) \\ y_{n+1} &= y_n + \left(\frac{k_1}{6} + \frac{k_2}{3} + \frac{k_3}{3} + \frac{k_4}{6}\right)\Delta t \end{aligned}$$

The Leapfrog

For a second order ODE: $\ddot{\mathbf{x}} = f(\mathbf{x})$

“Drift-Kick-Drift” version

$$\begin{aligned} x_{n+\frac{1}{2}} &= x_n + v_n \frac{\Delta t}{2} \\ v_{n+1} &= v_n + f(x_{n+\frac{1}{2}}) \Delta t \\ x_{n+1} &= x_{n+\frac{1}{2}} + v_{n+1} \frac{\Delta t}{2} \end{aligned}$$

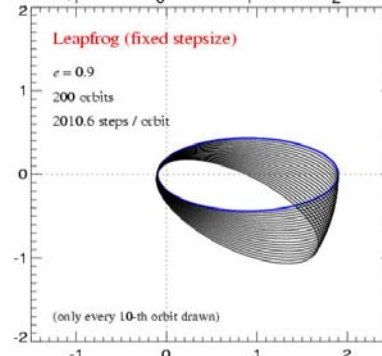
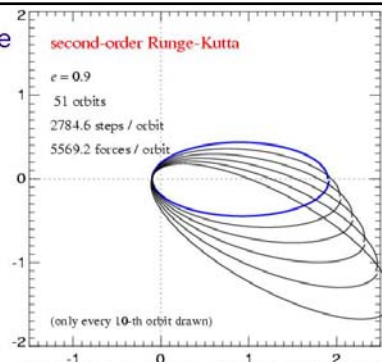
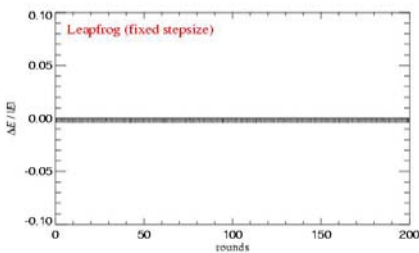
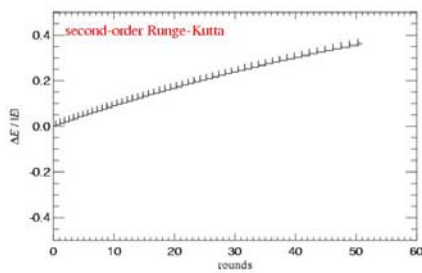
“Kick-Drift-Kick” version

$$\begin{aligned} v_{n+\frac{1}{2}} &= v_n + f(x_n) \frac{\Delta t}{2} \\ x_{n+1} &= x_n + v_{n+\frac{1}{2}} \frac{\Delta t}{2} \\ v_{n+1} &= v_{n+\frac{1}{2}} + f(x_{n+1}) \frac{\Delta t}{2} \end{aligned}$$

- 2nd order accurate
- symplectic
- can be rewritten into time-centred formulation

When compared with an integrator of the same order, the leapfrog is highly superior

INTEGRATING THE KEPLER PROBLEM



Nbody Dynamics: Historical

THE ASTROPHYSICAL JOURNAL

AN INTERNATIONAL REVIEW OF SPECTROSCOPY AND
ASTRONOMICAL PHYSICS

VOLUME 94

NOVEMBER 1941

NUMBER 3

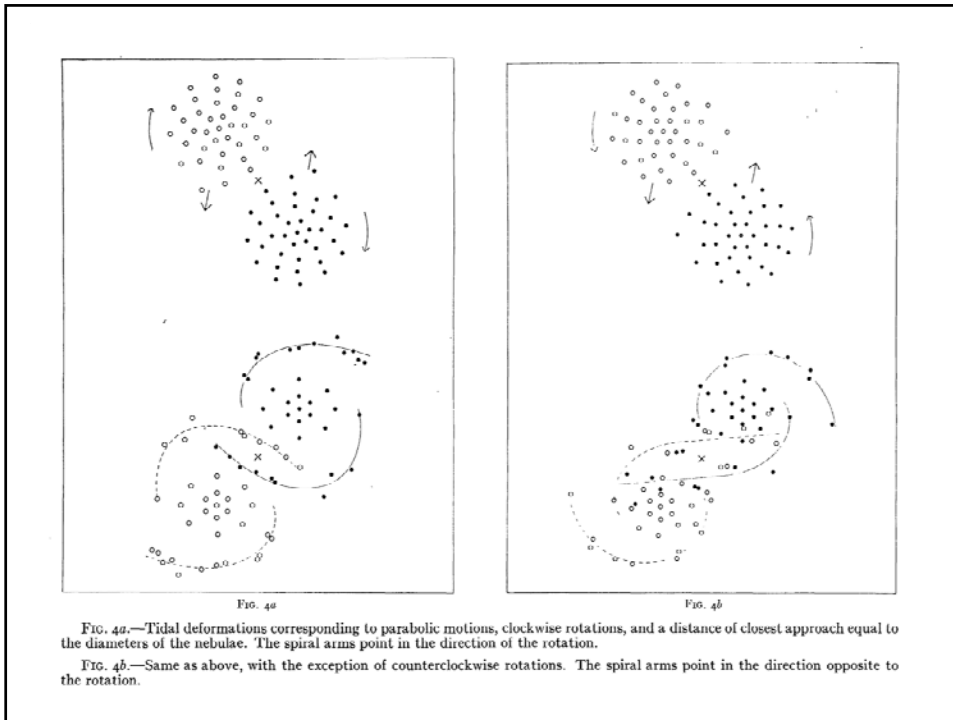
ON THE CLUSTERING TENDENCIES AMONG THE NEBULAE

II. A STUDY OF ENCOUNTERS BETWEEN LABORATORY MODELS OF
STELLAR SYSTEMS BY A NEW INTEGRATION PROCEDURE

ERIK HOLMBERG

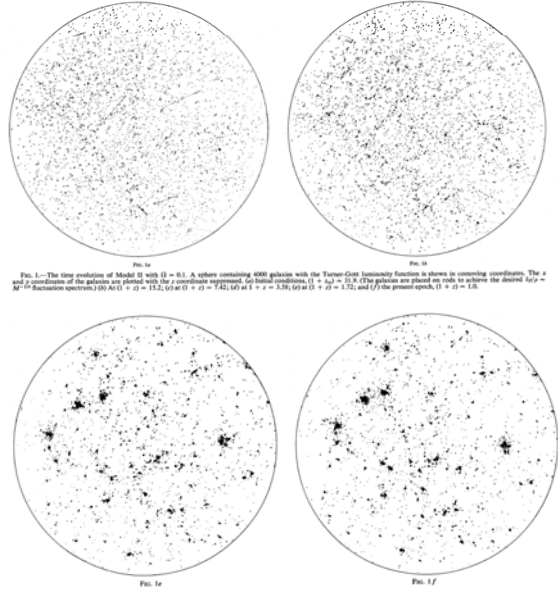
ABSTRACT

In a previous paper⁴ the writer discussed the possibility of explaining the observed clustering effects among extragalactic nebulae as a result of captures. The present investigation deals with the important problem of whether the loss of energy resulting from the tidal disturbances at a close encounter between two nebulae is large enough to effect a capture. The tidal deformations of two models of stellar systems, passing each other at a small distance, are studied by reconstructing, piece by piece, the orbits described by the individual mass elements. The difficulty of integrating the total gravitational force acting upon a certain element at a certain point of time is solved by replacing gravitation by light. The mass elements are represented by light-bulbs, the candle power being proportional to mass, and the total light is measured by a photocell (Fig. 1). The nebulae are assumed to have a flattened shape, and each is represented by 37 light-bulbs. It is found that the tidal deformations cause an increase in the attraction between the two objects, the increase reaching its maximum value when the nebulae are separating, i.e., after the passage. The resulting loss of energy (Fig. 6) is comparatively large and may, in favorable cases, effect a capture. The spiral arms developing during the encounter (Figs. 4) represent an interesting by-product of the investigation. The direction of the arms depends on the direction of rotation of the nebulae with respect to the direction of their space motions.



1979: Aarseth, Turner & Gott

- 1000 particles in spherical volume
- initial conditions: random/semi-random



1983: Klypin & Shandarin

- 32^3 particle in cubic volume
- initial conditions: 1st time proper cosmological Gaussian conditions: Zeldovich approximation
- PM particle-mesh simulation

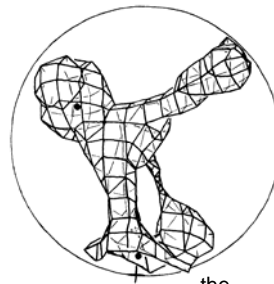
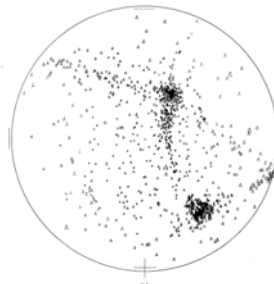
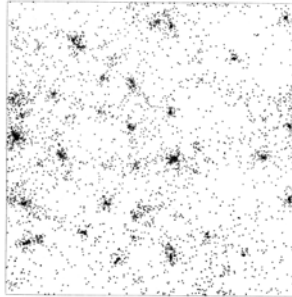


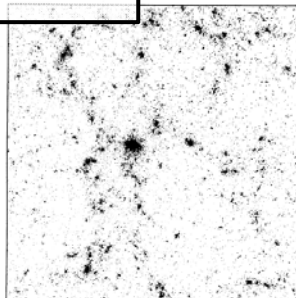
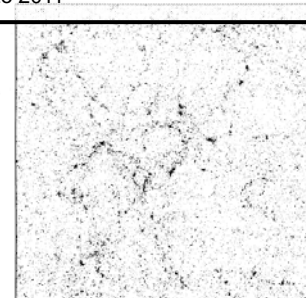
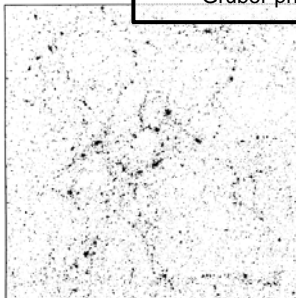
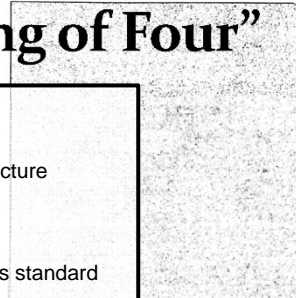
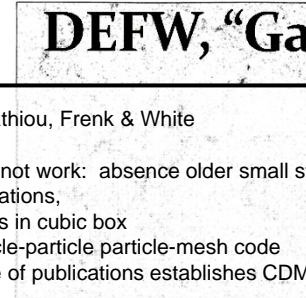
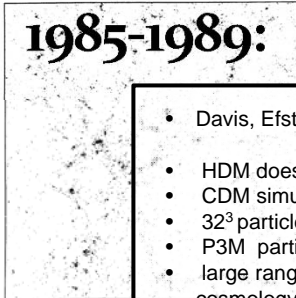
Figure 3. A small fragment of the particle distribution plotted in Fig. 2(b), when $a = 11.6 a_{\text{eq}}$. An equivalent to Fig. 2 here all particles in the sphere with radius $R = 50 h^{-1} \text{Mpc}$ are plotted. Every particle is depicted as a triangle whose size is inversely proportional to distance from an observer. The observer is placed at a distance $1.5 R$ from the center of the sphere.

the
"Cosmic Chicken"

1985-1989:

DEFW, "Gang of Four"

- Davis, Efstathiou, Frenk & White
- HDM does not work: absence older small structure
- CDM simulations,
- 32^3 particles in cubic box
- P3M particle-particle particle-mesh code
- large range of publications establishes CDM as standard cosmology
- Gruber prize 2011



1985-1989: DEFW, "Gang of Four"

- Davis, Efstathiou, Frenk & White
- HDM does not work: absence older small structure
- CDM simulations,
- 32^3 particles in cubic box
- P3M particle-particle particle-mesh code
- large range of publications establishes CDM as standard cosmology
- Gruber prize 2011

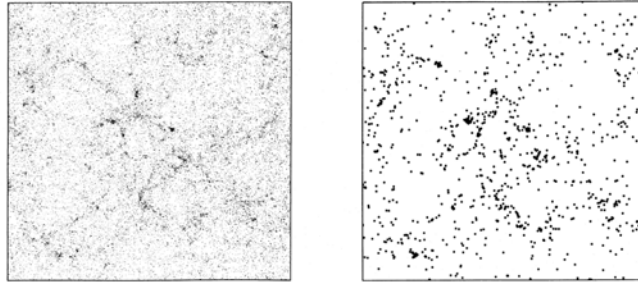


FIG. 16.—The projected distribution of all particles (left) and of the "galaxies" (right) in EdS1 at $a = 1.4$. The side of the box is $32.5h^{-1}$ Mpc. "Galaxies" are assumed to form only at the 2.5σ peaks of the linear density distribution.

1985-1989: DEFW, "Gang of Four"

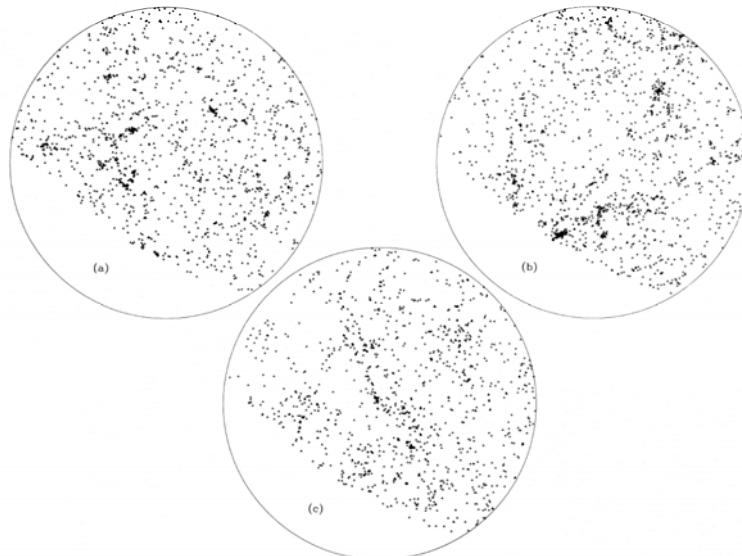
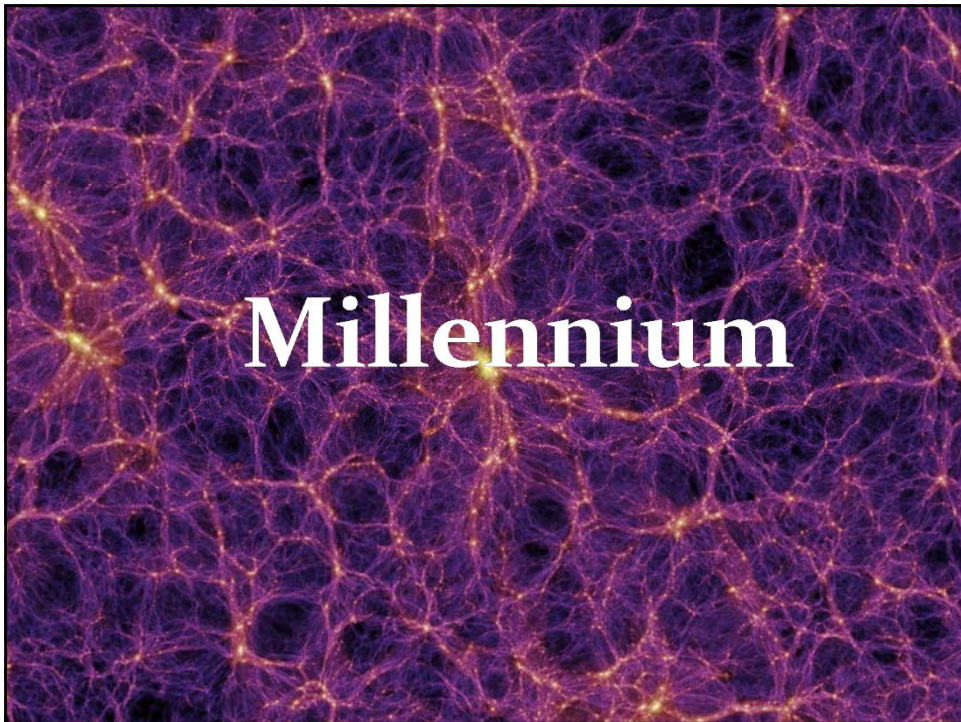
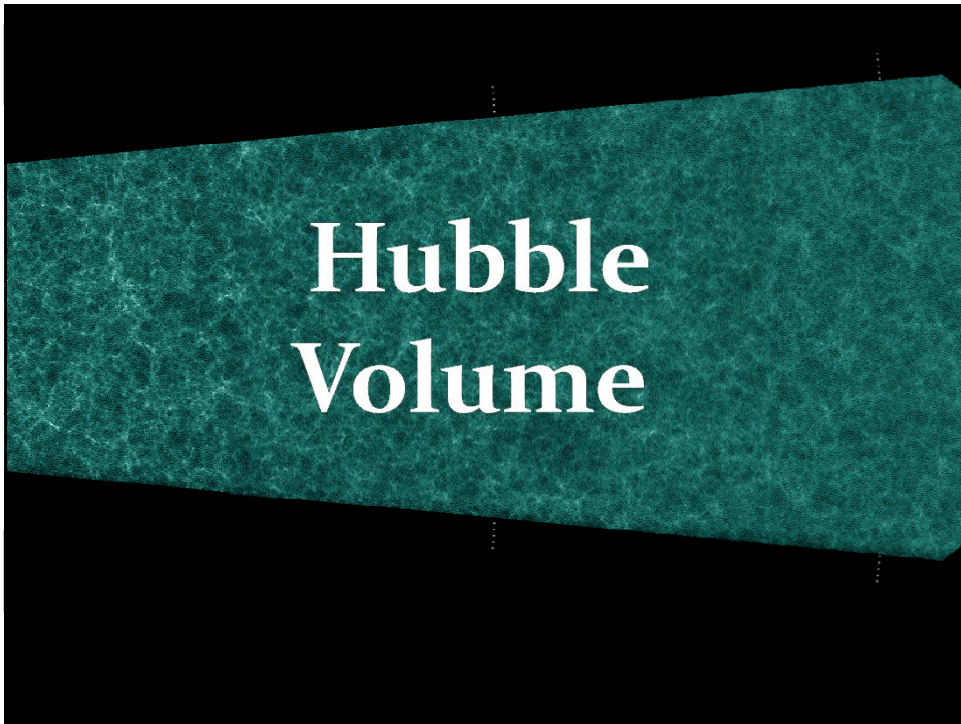
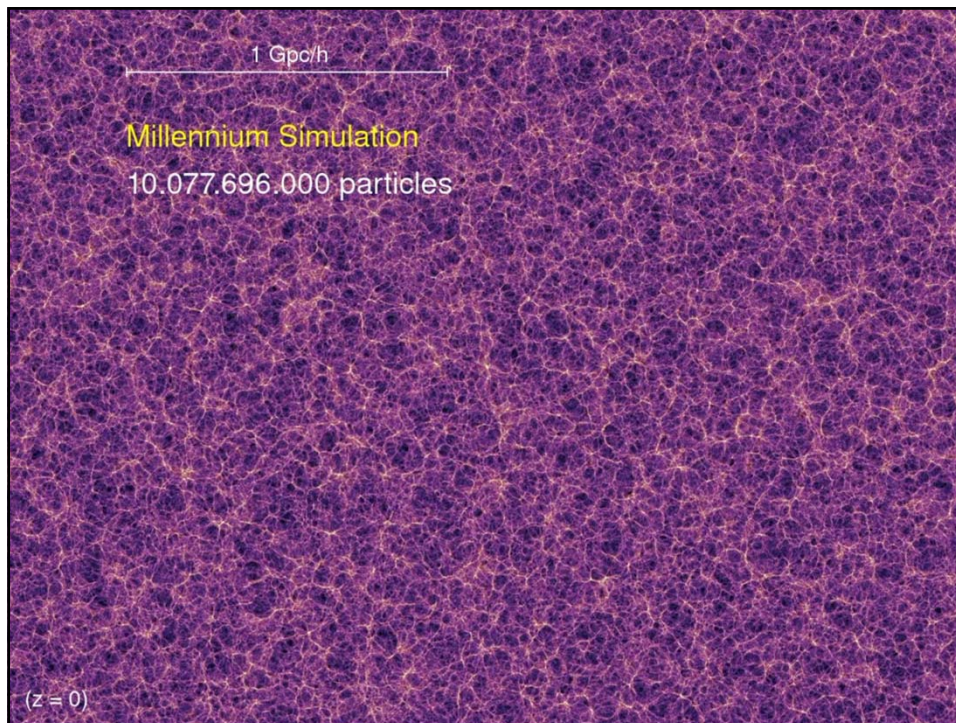


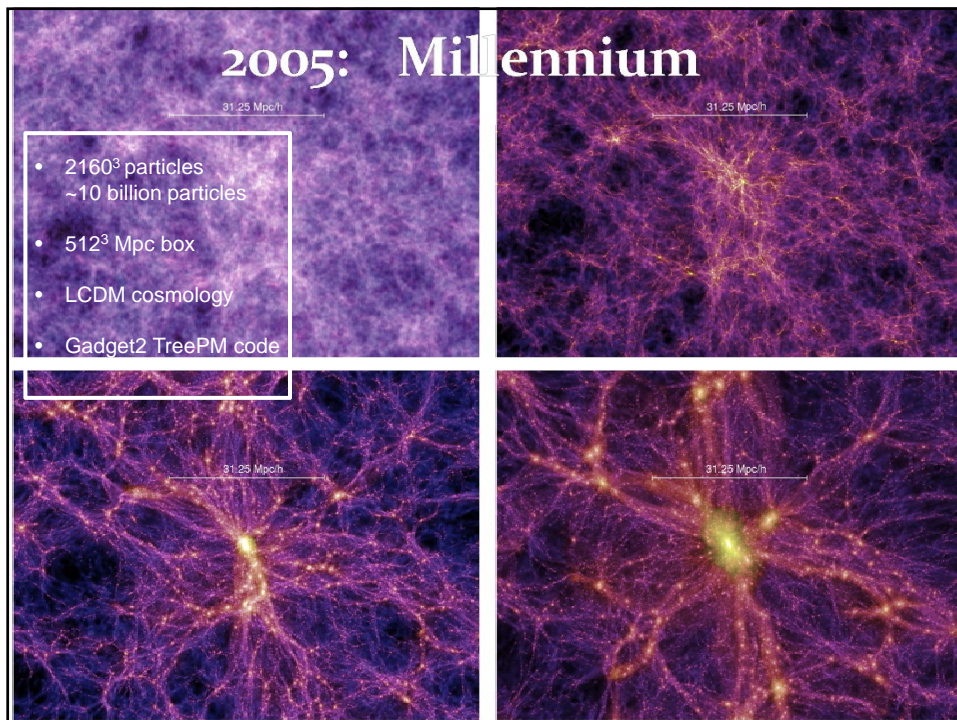
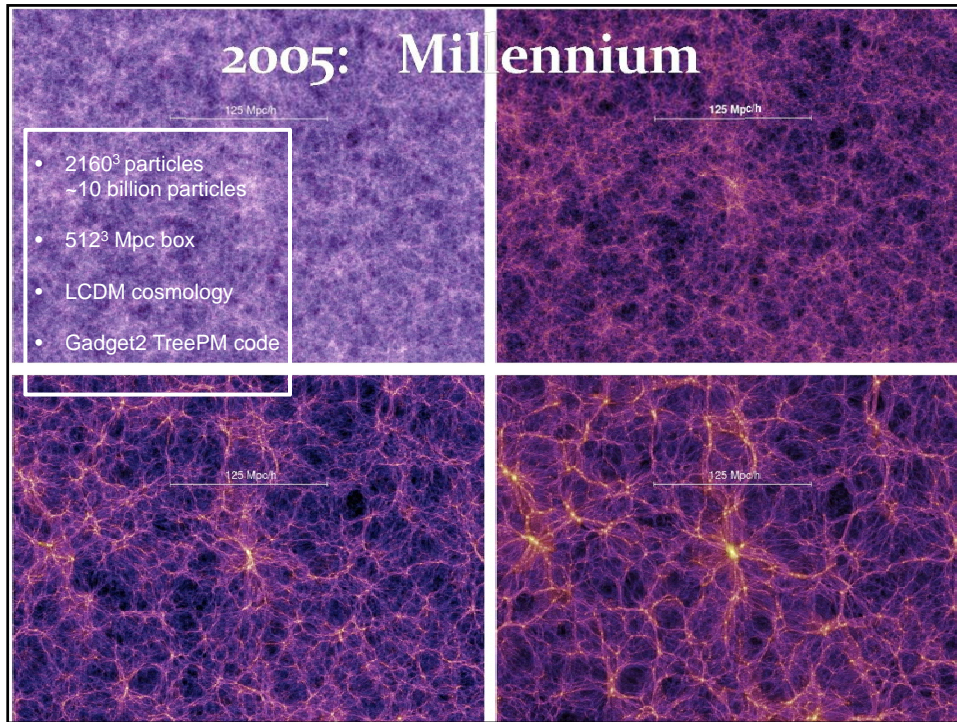
FIG. 12.—Redshift catalogs constructed from two open models (O2 and O3) are shown in (a) and (b) as projections onto the "sky." Particles were selected for inclusion in these catalogs in such a way as to mimic the northern CMA survey. The real data are shown in the same format in (c). These are equal area plots of the sky; the outer circle corresponds to Galactic latitude $+40^\circ$, while the empty regions correspond to declinations below 0° . In constructing the catalog from O3 shown in (b), the "observer" was purposely sited near a prominent cluster.

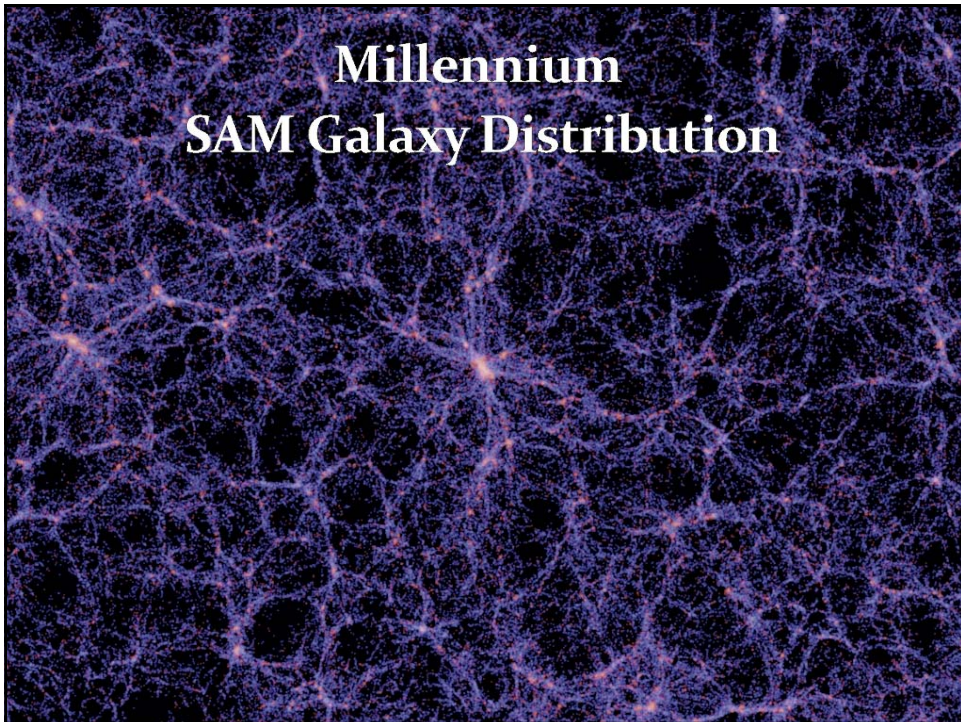


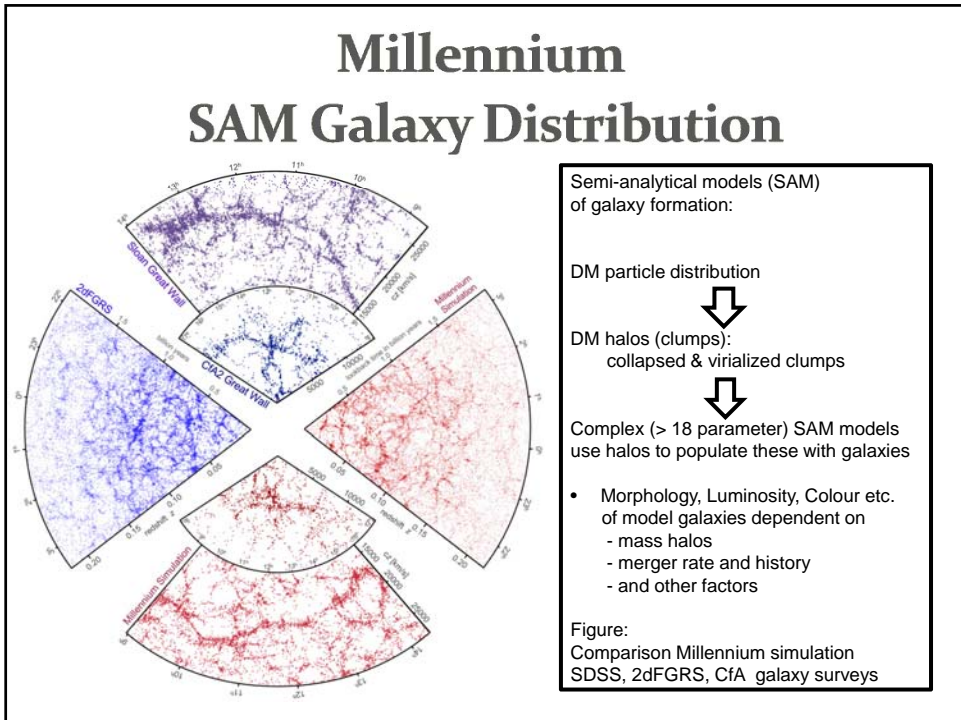


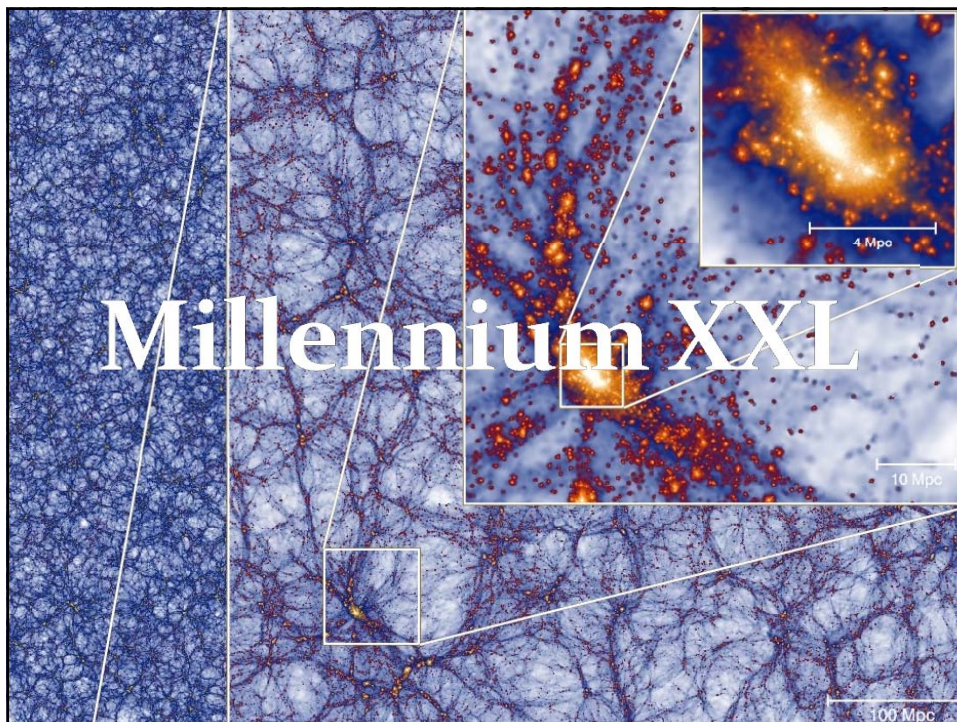
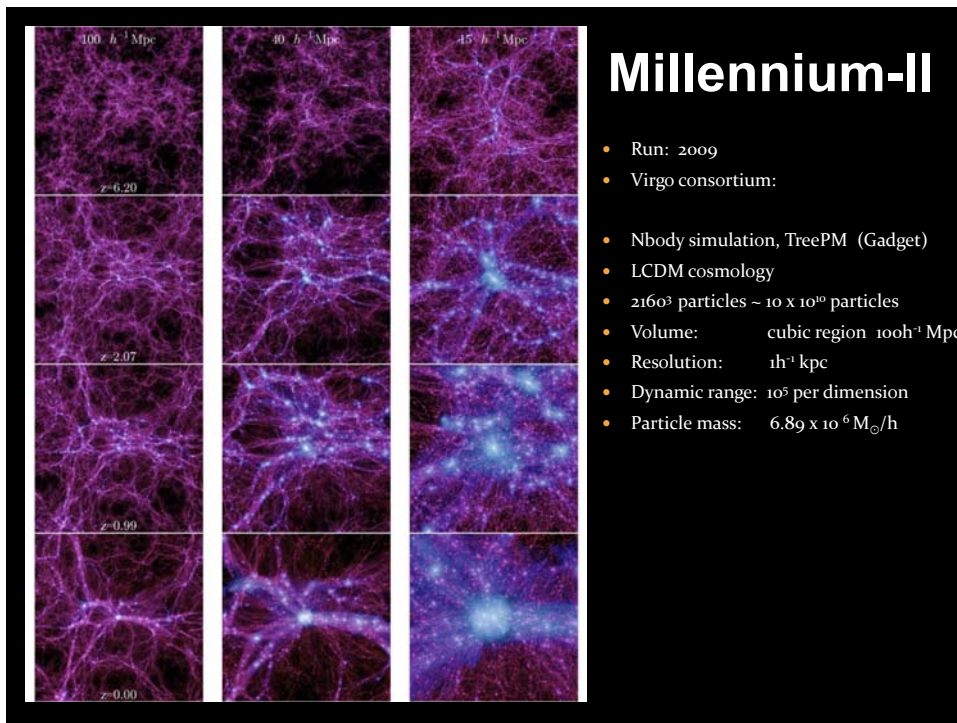
Millennium Simulation

- Run: 2005
- Virgo consortium: UK-Germany centered European consortium
- 2005-2014: 650 publications based on Millennium
- Nbody simulation, TreePM (Gadget2)
- LCDM cosmology
- 2160^3 particles $\sim 10 \times 10^{10}$ particles
- Volume: cubic region $500h^{-1}$ Mpc
- Resolution: $5h^{-1}$ kpc
- Dynamic range: 10^5 per dimension
- Data: 25 Terabyte
- Galaxy modelling by semi-analytical modelling
- 2×10^7 galaxies with mass $>$ LMC
- Public Database:
VO-oriented and SQL-queryable database (G. Lemson)



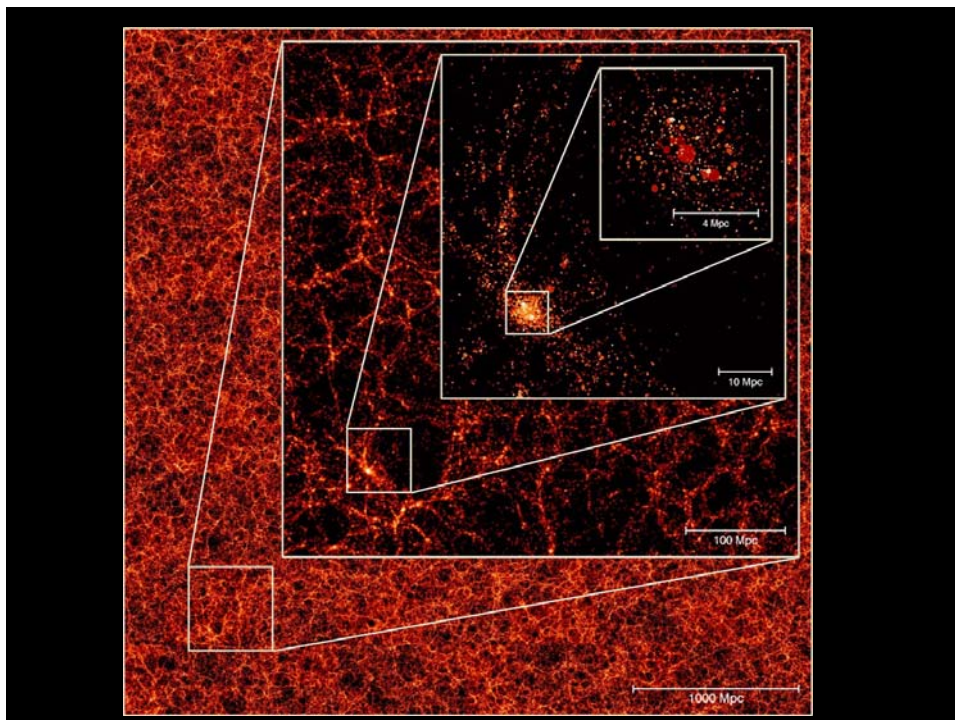






Millennium XXL Simulation

- Run: 2010
- Virgo consortium: UK-Germany centered European consortium
- First multi - 100 billion particle simulation
- Nbody simulation, TreePM (Gadget2)
- LCDM cosmology
- 6720^3 particles $\sim 300 \times 10^{10}$ particles
- Volume: cubic region 4.1 Gpc
216 volume Millennium
27000 volumes Millennium-II
- Run on JUROPA supercomputer,
12,000 cores, 300 years CPU time, 30 Terabyte RAM
- Data: 100 Terabyte
- Galaxy modelling by semi-analytical modelling
- 700×10^6 galaxies at $z=0$



PM:

Particle-Mesh

The particle-mesh method

Poisson's equation can be solved in real-space by a convolution of the density field with a Green's function.

$$\Phi(\mathbf{x}) = \int g(\mathbf{x} - \mathbf{x}') \rho(\mathbf{x}) d\mathbf{x}'$$

Example for vacuum boundaries:

$$\Phi(\mathbf{x}) = -G \int \frac{\rho(\mathbf{x})}{|\mathbf{x} - \mathbf{x}'|} d\mathbf{x}' \quad g(\mathbf{x}) = -\frac{G}{|\mathbf{x}|}$$

In Fourier-space, the convolution becomes a simple multiplication!

$$\hat{\Phi}(\mathbf{k}) = \hat{g}(\mathbf{k}) \cdot \hat{\rho}(\mathbf{k})$$

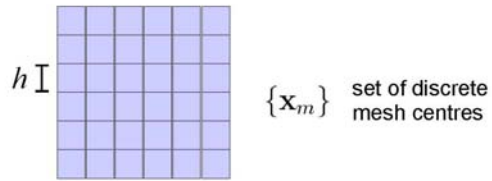
→ Solve the potential in these steps:

- (1) FFT forward of the density field
- (2) Multiplication with the Green's function
- (3) FFT backwards to obtain potential

The four steps of the PM algorithm

- (a) Density assignment
- (b) Computation of the potential
- (c) Determination of the force field
- (d) Assignment of forces to particles

Density assignment



Give particles a "shape" $S(x)$. Then to each mesh cell, we assign the fraction of mass that falls into this cell. The overlap for a cell is given by:

$$W(\mathbf{x}_m - \mathbf{x}_i) = \int_{\mathbf{x}_m - \frac{h}{2}}^{\mathbf{x}_m + \frac{h}{2}} S(\mathbf{x}' - \mathbf{x}_i) d\mathbf{x}' = \int \Pi\left(\frac{\mathbf{x}' - \mathbf{x}_m}{h}\right) S(\mathbf{x}' - \mathbf{x}_i) d\mathbf{x}'$$




The assignment function is hence the convolution:

$$W(\mathbf{x}) = \Pi\left(\frac{\mathbf{x}}{h}\right) \star S(\mathbf{x}) \quad \text{where} \quad \Pi(x) = \begin{cases} 1 & \text{for } |x| \leq \frac{1}{2} \\ 0 & \text{otherwise} \end{cases}$$

The density on the mesh is then a sum over the contributions of each particle as given by the assignment function:

$$\rho(\mathbf{x}_m) = \frac{1}{h^3} \sum_{i=1}^N m_i W(\mathbf{x}_i - \mathbf{x}_m)$$

Commonly used particle shape functions and assignment schemes

Name	Shape function $S(x)$	# of cells involved	Properties of force
NGP Nearest grid point	 $\delta(\mathbf{x})$	$1^3 = 1$	piecewise constant in cells
CIC Clouds in cells	 $\frac{1}{h^3} \Pi\left(\frac{\mathbf{x}}{h}\right) \star \delta(\mathbf{x})$	$2^3 = 8$	piecewise linear, continuous
TSC Triangular shaped clouds	 $\frac{1}{h^3} \Pi\left(\frac{\mathbf{x}}{h}\right) \star \frac{1}{h^3} \Pi\left(\frac{\mathbf{x}}{h}\right)$	$3^3 = 27$	continuous first derivative

Note: For interpolation of the grid to obtain the forces, the same assignment function needs to be used to ensure momentum conservation. (In the CIC case, this is identical to tri-linear interpolation.)

Advantages and disadvantages of the PM-scheme

Pros: **SPEED** and simplicity

- Cons:**
- Spatial force resolution limited to mesh size.
 - Force errors somewhat anisotropic on the scale of the cell size



serious problem:

cosmological simulations cluster strongly and have a very large dynamic range

cannot make the PM-mesh fine enough and resolve internal structure of halos as well as large cosmological scales



we need a method to increase the **dynamic range** available in the force calculation

P₃M:

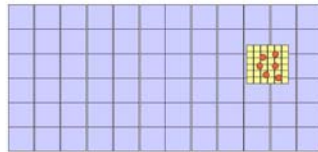
Particle-Particle Particle-Mesh

Particle-Particle PM schemes (P³M)

Idea: Supplement the PM force with a direct summation short-range force at the scale of the mesh cells. The particles in cells are linked together by a chaining list.

Offers much higher dynamic range, but becomes slow when clustering sets in.

In AP³M, mesh-refinements are placed on clustered regions



Can avoid clustering slow-down, but has higher complexity and ambiguities in mesh placement

Codes that use AP³M: **HYDRA** (Couchman)

DEFW:

Davis –Efstathiou-Frenk-White

‘the gang of four’

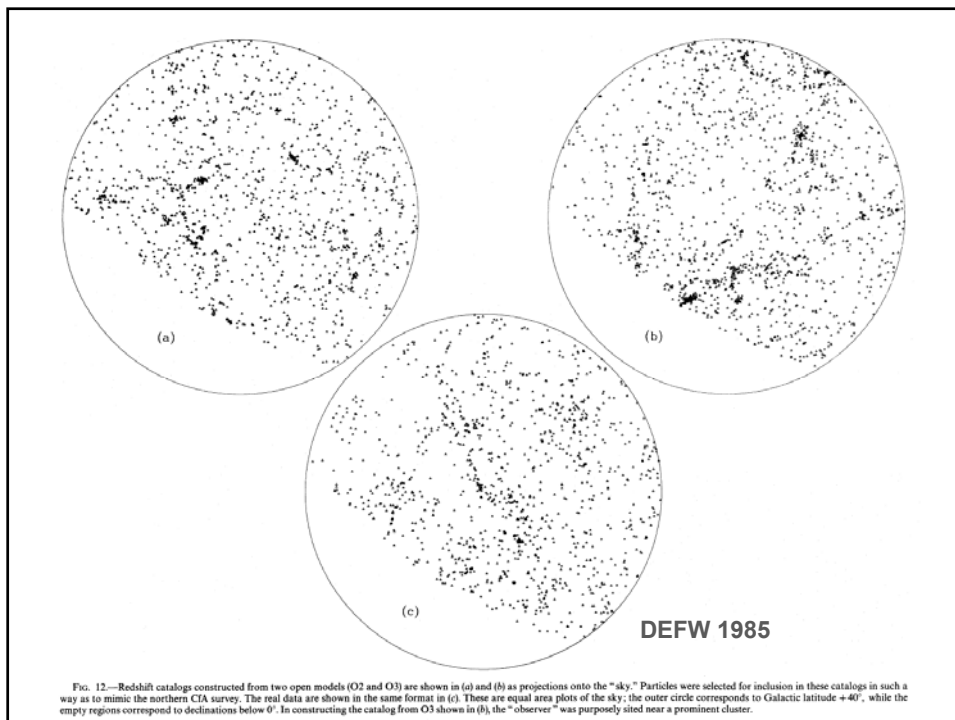
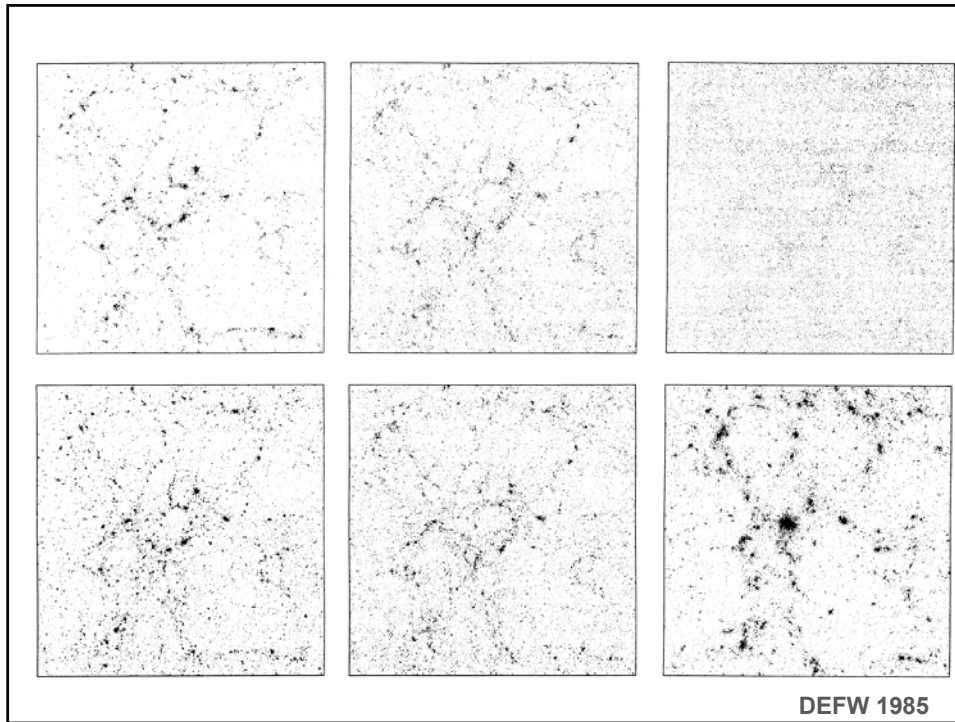
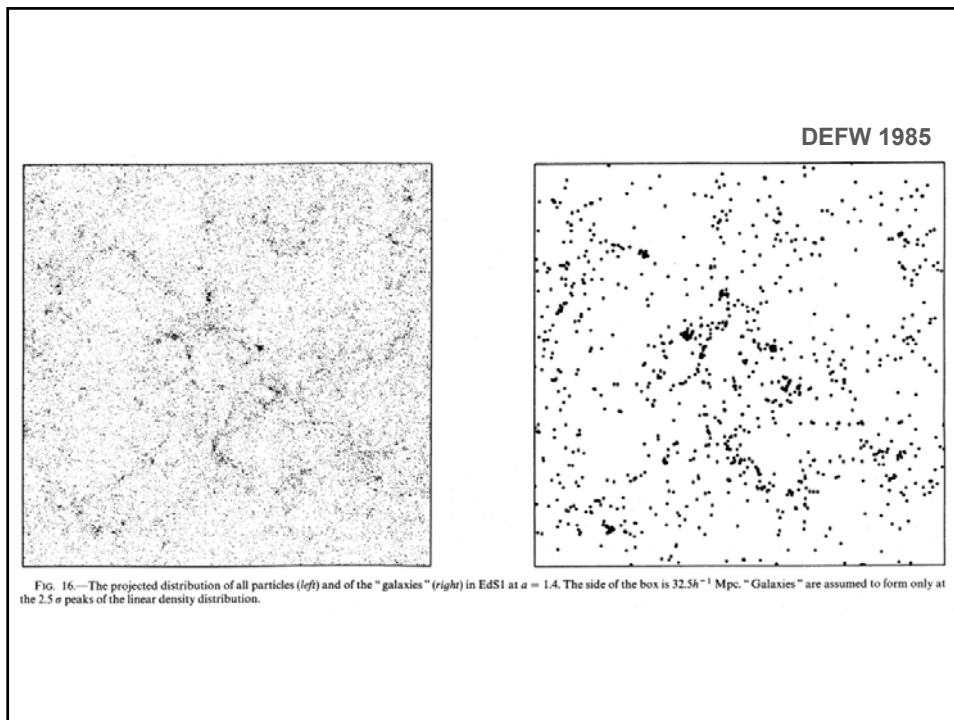


FIG. 12.—Redshift catalogs constructed from two open models (O2 and O3) are shown in (a) and (b) as projections onto the “sky.” Particles were selected for inclusion in these catalogs in such a way as to mimic the northern CIA survey. The real data are shown in the same format in (c). These are equal area plots of the sky; the outer circle corresponds to Galactic latitude $+40^\circ$, while the empty regions correspond to declinations below 0° . In constructing the catalog from O3 shown in (b), the “observer” was purposely sited near a prominent cluster.



Tree Algorithms

Gravity is the driving force for structure formation in the universe

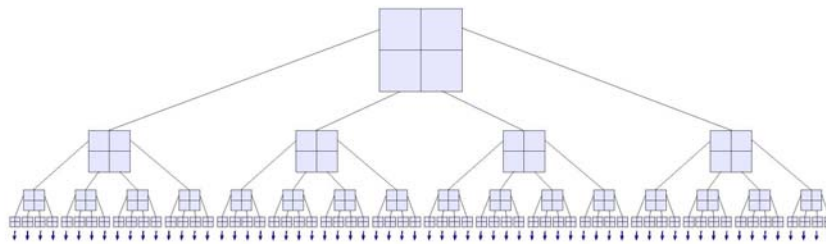
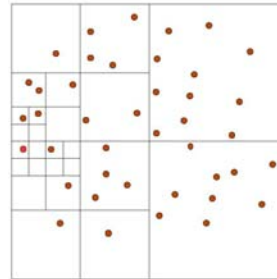
HIERARCHICAL TREE ALGORITHMS

The N^2 -scaling of direct summation puts serious limitations on N ...

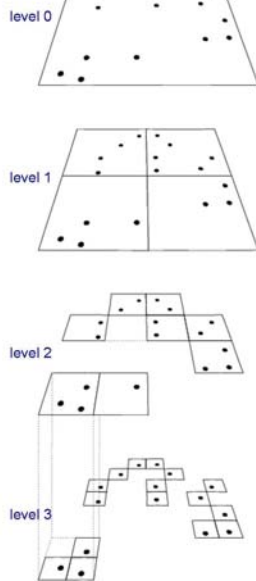
But we want $N \sim 10^6-10^{10}$ for collisionless dynamics of dark matter !

Idea: Group distant particles together, and use their multipole expansion.

► Only $\sim \log(N)$ force terms per particle.



Oct-tree in two dimensions



Tree algorithms

Idea: Use hierarchical multipole expansion to account for distant particle groups

$$\Phi(\mathbf{r}) = -G \sum_i \frac{m_i}{|\mathbf{r} - \mathbf{x}_i|}$$

We expand:

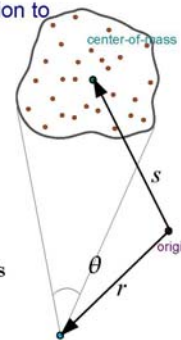
$$\frac{1}{|\mathbf{r} - \mathbf{x}_i|} = \frac{1}{|(\mathbf{r} - \mathbf{s}) - (\mathbf{x}_i - \mathbf{s})|}$$

for $|\mathbf{x}_i - \mathbf{s}| \ll |\mathbf{r} - \mathbf{s}|$ $\mathbf{y} \equiv \mathbf{r} - \mathbf{s}$

and obtain:

$$\frac{1}{|\mathbf{y} + \mathbf{s} - \mathbf{x}_i|} = \frac{1}{|\mathbf{y}|} - \frac{\mathbf{y} \cdot (\mathbf{s} - \mathbf{x}_i)}{|\mathbf{y}|^3} + \frac{1}{2} \frac{\mathbf{y}^T [3(\mathbf{s} - \mathbf{x}_i)(\mathbf{s} - \mathbf{x}_i)^T - \mathbf{I}(\mathbf{s} - \mathbf{x}_i)^2] \mathbf{y}}{|\mathbf{y}|^5} + \dots$$

the dipole term vanishes when summed over all particles in the group



The multipole moments are computed for each node of the tree

Monopole moment:

$$M = \sum_i m_i$$

Quadrupole tensor:

$$Q_{ij} = \sum_k m_k \left[3(\mathbf{x}_k - \mathbf{s})_i (\mathbf{x}_k - \mathbf{s})_j - \delta_{ij} (\mathbf{x}_k - \mathbf{s})^2 \right]$$

Resulting potential/force approximation:

$$\Phi(\mathbf{r}) = -G \left[\frac{M}{|\mathbf{y}|} + \frac{1}{2} \frac{\mathbf{y}^T \mathbf{Q} \mathbf{y}}{|\mathbf{y}|^5} \right]$$

For a single force evaluation, not N single-particle forces need to be computed, but **only of order $\log(N)$ multipoles**, depending on opening angle.

- The tree algorithm has no intrinsic restrictions for its dynamic range
- force accuracy can be conveniently adjusted to desired level
- the speed does depend only very weakly on clustering state
- geometrically flexible, allowing arbitrary geometries

TreePM

mixing Treecode with PM

Particularly at high redshift, it is expensive to obtain accurate forces with the tree-algorithm

THE TREE-PM FORCE SPLIT

Periodic peculiar potential

$$\nabla^2 \phi(\mathbf{x}) = 4\pi G[\rho(\mathbf{x}) - \bar{\rho}] = 4\pi G \sum_{\mathbf{n}} \sum_i m_i \left[\delta(\mathbf{x} - \mathbf{x}_i - \mathbf{n}L) - \frac{1}{L^3} \right]$$

Idea: Split the potential (of a single particle) in Fourier space into a long-range and a short-range part, and compute them separately with PM and TREE algorithms, respectively.

Poisson equation in Fourier space: $\phi_{\mathbf{k}} = -\frac{4\pi G}{\mathbf{k}^2} \rho_{\mathbf{k}} \quad (\mathbf{k} \neq 0)$

$$\phi_{\mathbf{k}}^{\text{long}} = \phi_{\mathbf{k}} \exp(-\mathbf{k}^2 r_s^2)$$

$$\phi_{\mathbf{k}}^{\text{short}} = \phi_{\mathbf{k}} [1 - \exp(-\mathbf{k}^2 r_s^2)]$$

Solve with PM-method

- CIC mass assignment
- FFT
- multiply with kernel
- FFT backwards
- Compute force with 4-point finite difference operator
- Interpolate forces to particle positions

FFT to real space $\phi(r) = -\frac{Gm}{r} \operatorname{erfc}\left(\frac{r}{2r_s}\right)$

Solve in real space with TREE

The maximum size of a TreePM simulation with *Lean-GADGET-II* is essentially memory bound

A HIGHLY MEMORY EFFICIENT VERSION OF GADGET-II

Particle Data

44 bytes / particle

Tree storage

40 bytes / particle

FFT workspace

24 bytes / mesh-cell

Not needed concurrently!

Special code version

84 bytes / particle

Lean-GADGET-II needs:

(Assuming 1.5 mesh-cells/particle)

Simulation Set-up:

- Particle number: $2160^3 = 10.077.696.000 = \sim 10^{10}$ particles
- Boxsize: $L = 500 h^{-1} \text{ Mpc}$
- Particle mass: $m_p = 8.6 \times 10^8 h^{-1} M_{\odot}$
- Spatial resolution: $5 h^{-1} \text{ kpc}$
- Size of FFT: $2560^3 = 16.777.216.000 = \sim 17$ billion cells

Minimum memory requirement of simulation code

~840 GByte

Compared to Hubble-Volume simulation:

- > 2000 times better mass resolution
- 10 times larger particle number
- 13 better spatial resolution

Moving Mesh:

Arepo & TESS

A finite volume discretization of the Euler equations on a moving mesh can be readily defined

THE EULER EQUATIONS AS HYPERBOLIC SYSTEM OF CONSERVATION LAWS

Euler equations

$$\frac{\partial \mathbf{U}}{\partial t} + \nabla \cdot \mathbf{F} = 0$$

State vector

$$\mathbf{U} = \begin{pmatrix} \rho \\ \rho \mathbf{v} \\ \rho e \end{pmatrix}$$

Flux vector

$$\mathbf{F}(\mathbf{U}) = \begin{pmatrix} \rho \mathbf{v} \\ \rho \mathbf{v} \mathbf{v}^T + P \\ (\rho e + P) \mathbf{v} \end{pmatrix}$$

$$e = u + v^2/2$$

Equation of state: $P = (\gamma - 1)\rho u$

Discretization in terms of a number of finite volume cells:

Cell averages

$$\mathbf{Q}_i = \begin{pmatrix} M_i \\ \mathbf{p}_i \\ E_i \end{pmatrix} = \int_{V_i} \mathbf{U} dV$$

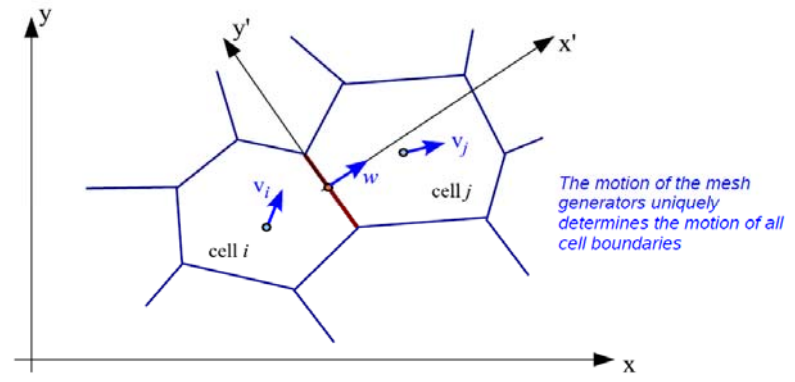
Evolution equation

$$\frac{d\mathbf{Q}_i}{dt} = - \int_{\partial V_i} [\mathbf{F}(\mathbf{U}) - \mathbf{U} \mathbf{w}^T] d\mathbf{n}$$

But how to compute the fluxes through cell surfaces?

The fluxes are calculated with an exact Riemann solver in the frame of the moving cell boundary

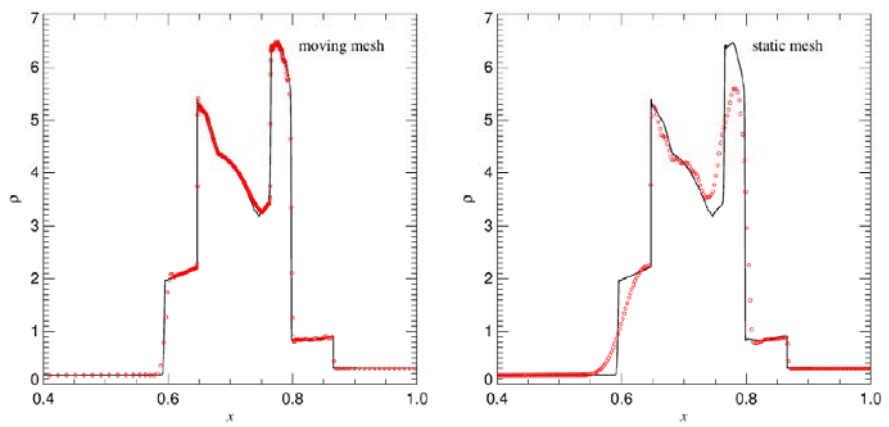
SKETCH OF THE FLUX CALCULATION

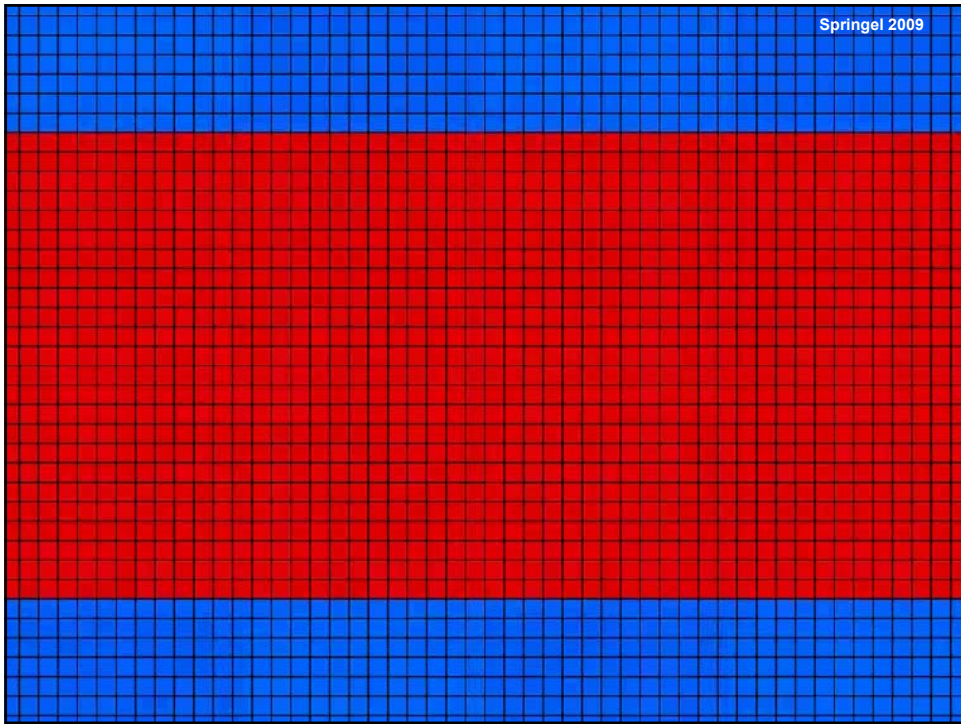


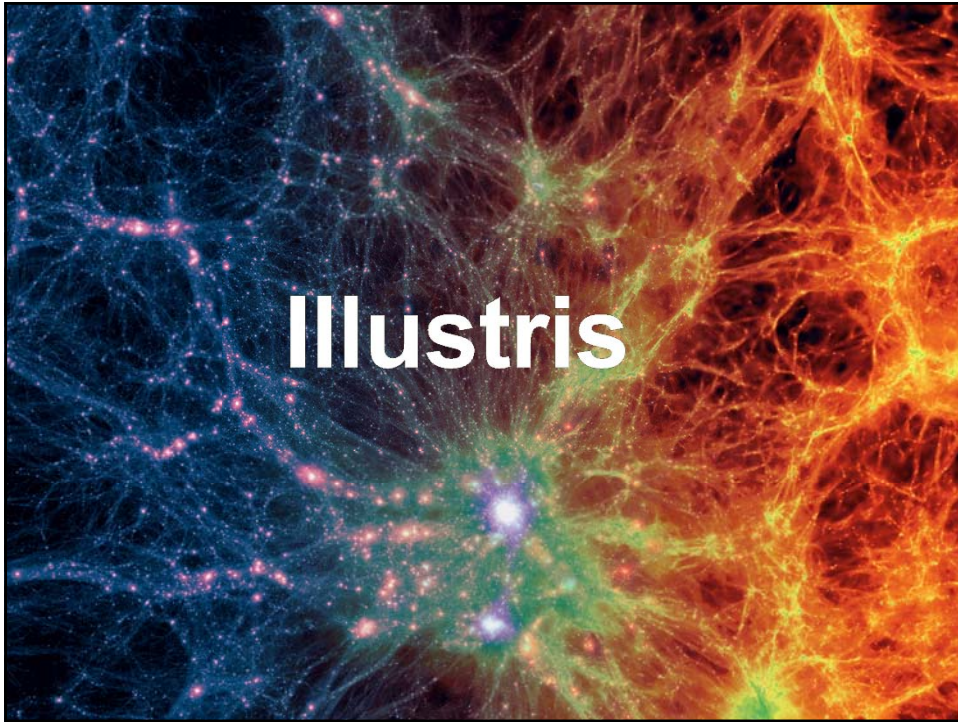
State left of cell face	State right of cell face			
$\begin{pmatrix} \rho_L \\ v_L \\ P_L \end{pmatrix}$	$\begin{pmatrix} \rho_R \\ v_R \\ P_R \end{pmatrix}$	$\xrightarrow{\text{Riemann solver (in frame of cell face)}}$	$\begin{pmatrix} \rho \\ v \\ p \end{pmatrix}$	$\rightarrow F(U)$

The moving-mesh code deals well with problems that involve complicated shock interactions

WOODWARD & COLELLA'S INTERACTING DOUBLE BLAST PROBLEM



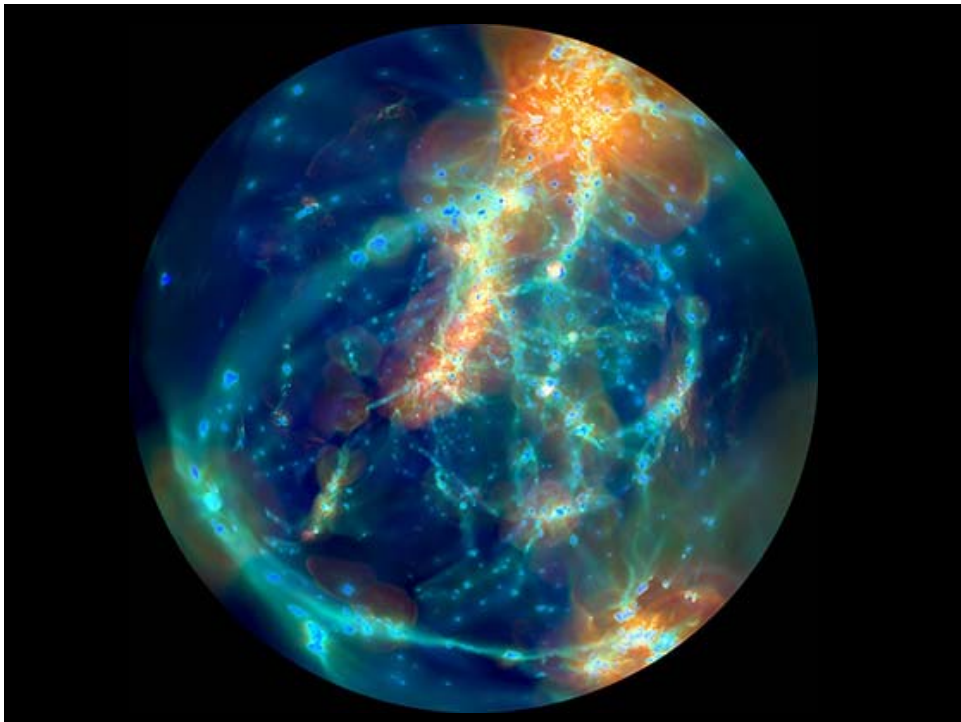
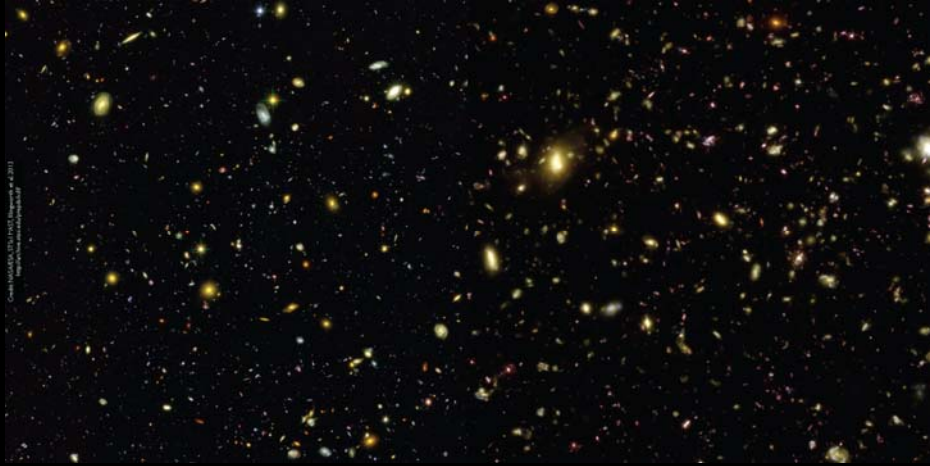


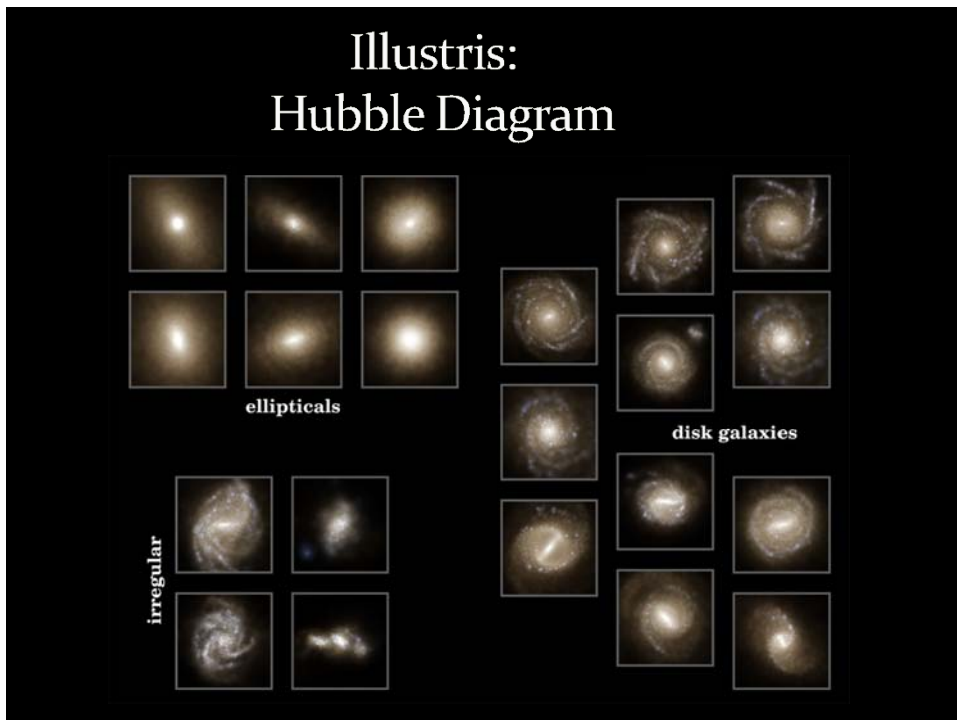
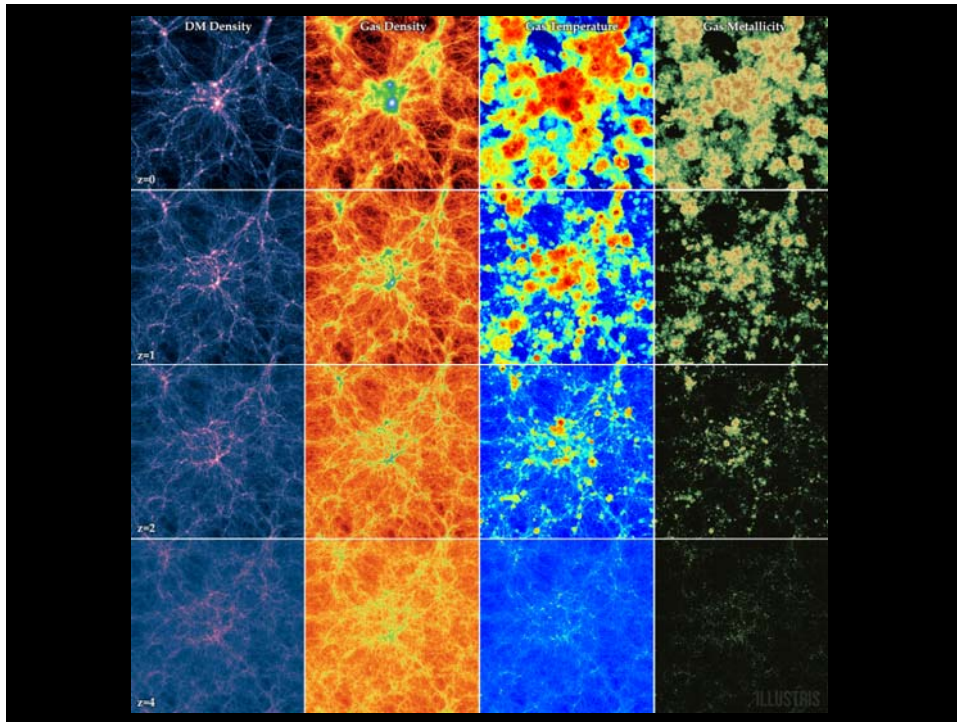


Illustris Simulation

- Run: 2013-2014
- First multi - 100 billion particle simulation
- Arepo adaptive-grid (Voronoi) Nbody+hydro simulations
- LCDM cosmology
- 6720^3 particles $\sim 300 \times 10^{10}$ particles
- Run on various supercomputers (France, Germany, USA),
8192 cores, 19 million CPU hours, 25 Terabyte RAM
- Data: 230 Terabyte

Illustris: HUDF, real vs. simulated





Phase-Space Dynamics

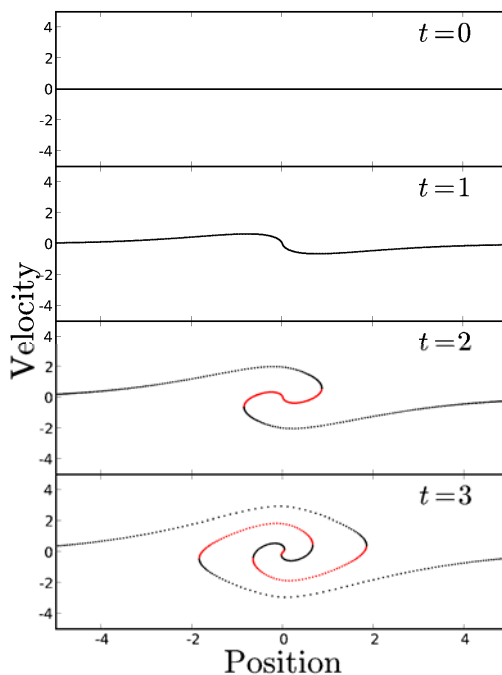
Phase Space Evolution

Dark Matter Phase Space sheet:

3-D structure projection of a folding DM phase space sheet
In 6-D phase space

- Shandarin 2010, 2011
- Neyrinck et al. 2011, 2012
- Origami
- Abel et al. 2011

Evolving matter distribution in
position-velocity space – 1D

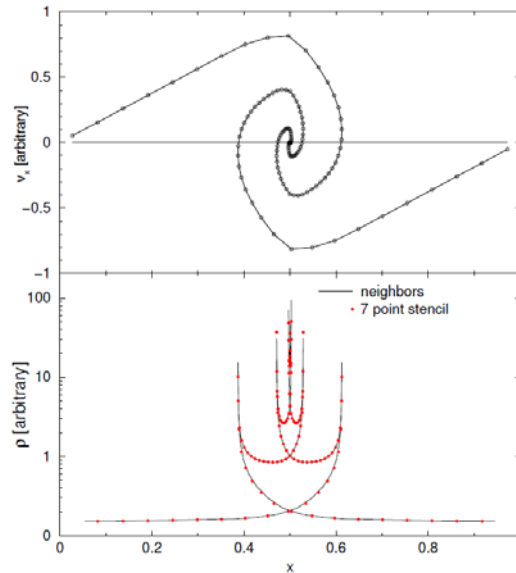


Phase Space Evolution

Phase space:
Velocity vs. Position



Density:
 $\rho(\vec{x}, t) = \int f(\vec{x}, \vec{v}, t) d\vec{v}$



Lagrangian-Eulerian Phase Space

To follow evolving phase-space of cosmic structure, it is sometimes insightful to consider a coordinate transformation of 6D phase-space:

Eulerian coordinates \vec{x} and Eulerian coordinates \vec{q} of a mass element:

$$f(\vec{x}, \vec{q})$$

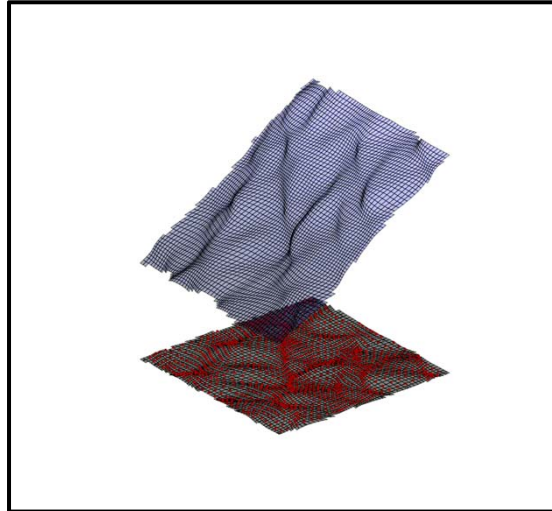
Note that in Zeldovich approximation, the velocity of a mass element is:

$$\vec{v}(\vec{q}, t) = -a(t)D(t)f(\Omega) \vec{\nabla}\Phi(\vec{q})$$

Tessellation Deformation & Phase Space Projection

Translation towards Multi-D space:

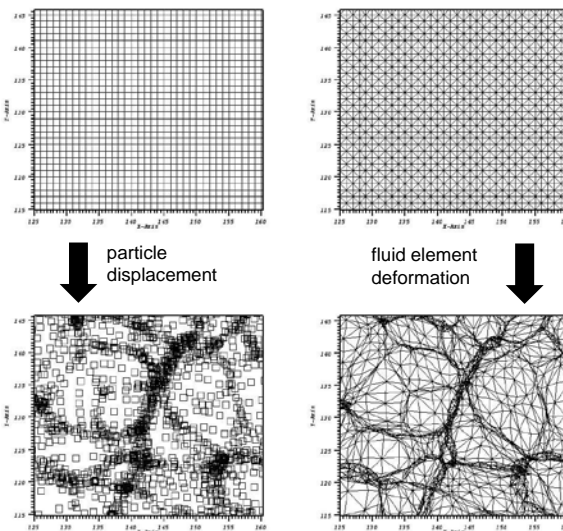
- Look at deformation of initial tessellation
- each tessellation cell represents matter cell
- evolution deforms cell
- once cells start to overlap, manifestation of different phase-space matter streams



Tessellation Deformation & Phase Space Projection

Translation towards Multi-D space:

- Look at deformation of initial tessellation
- each tessellation cell represents matter cell
- evolution deforms cell
- once cells start to overlap, manifestation of different phase-space matter streams

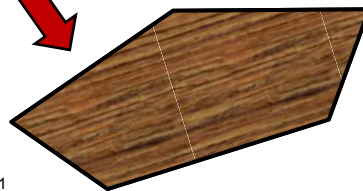
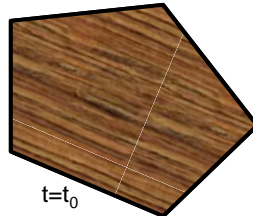


Tessellation Deformation & Phase Space Projection

Translation towards Multi-D space:

- Look at deformation of initial tessellation
- each tessellation cell represents matter cell
- evolution deforms cell

Monostream Density Evolution



Conservation of mass (continuity eqn.):

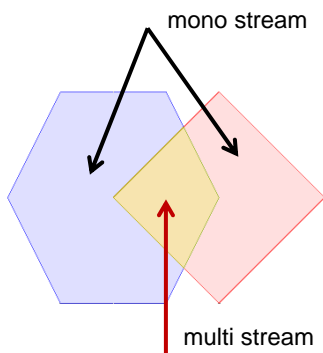
$$\rho(\vec{x}, t) = |J(\vec{x}, \vec{q})|^{-1} \rho(\vec{q}) = \left| \frac{\partial \vec{x}}{\partial \vec{q}} \right|^{-1} \rho(\vec{q})$$



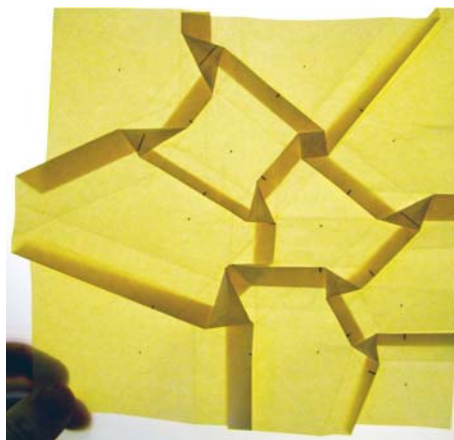
$$\rho(\vec{x}, t) = \frac{V_0}{V_1} \rho(\vec{q}, t_0)$$

(Cosmic) ORIGAMI

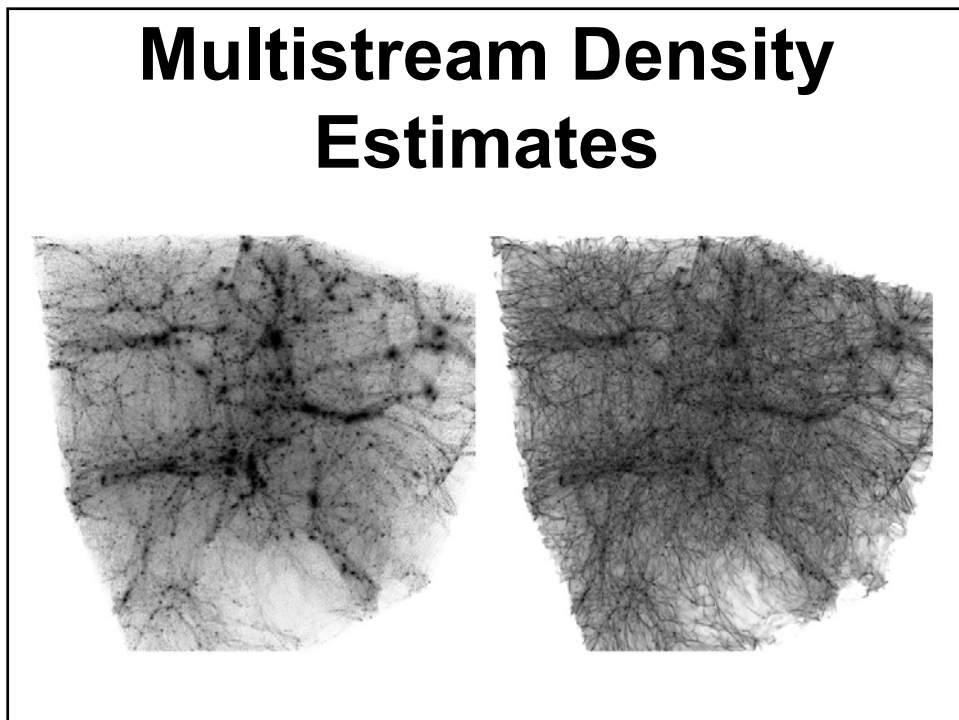
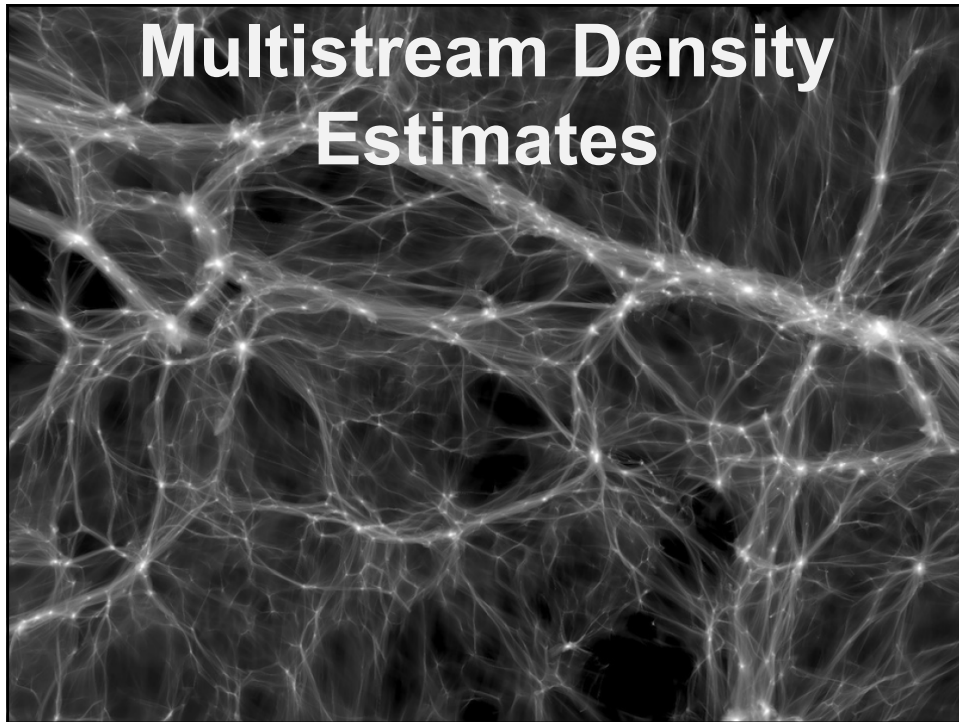
Evolution of dynamical system:
Phase-space folding – Cosmic Origami



$$\rho_{total}(\vec{x}, t_1) = \sum_i \frac{V_{0i}}{V_{1i}} \rho(\vec{q}_i, t_0)$$



Mark Neyrinck



Cosmic Web Stream Density

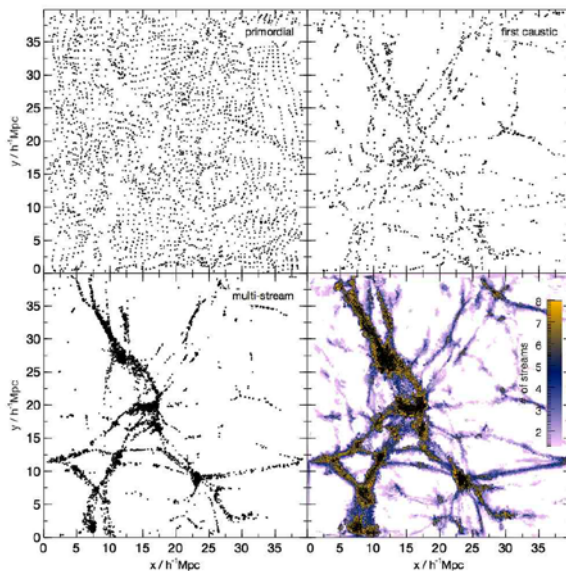
Translation towards
Multi-D space:

Density of
dark matter streams:

- # phase space folds

=

locally overlapping
tessellation cells



SPH

Smooth Particle Hydrodynamics

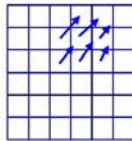
What is smoothed particle hydrodynamics?

DIFFERENT METHODS TO DISCRETIZE A FLUID

Eulerian

discretize space

representation on a mesh
(volume elements)



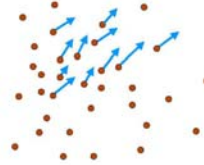
principle advantage:

high accuracy (shock capturing), low numerical viscosity

Lagrangian

discretize mass

representation by fluid elements
(particles)



principle advantage:

resolutions adjusts automatically to the flow



The baryons in the universe can be modelled as an *ideal* gas

BASIC HYDRODYNAMICAL EQUATIONS

Euler equation:
$$\frac{d\mathbf{v}}{dt} = -\frac{\nabla P}{\rho} - \nabla\Phi$$

Continuity equation:
$$\frac{d\rho}{dt} + \rho\nabla \cdot \mathbf{v} = 0$$

First law of thermodynamics:
$$\frac{du}{dt} = -\frac{P}{\rho}\nabla \cdot \mathbf{v} - \frac{\Lambda(u, \rho)}{\rho}$$

Equation of state of ideal monoatomic gas:
$$P = (\gamma - 1)\rho u, \quad \gamma = 5/3$$

Kernel interpolation is used in smoothed particle hydrodynamics (SPH) to build continuous fluid quantities from discrete tracer particles

DENSITY ESTIMATION IN SPH BY MEANS OF ADAPTIVE KERNEL ESTIMATION

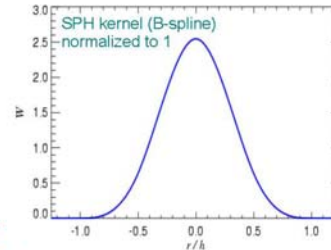
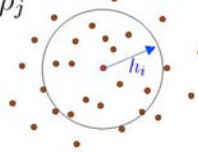
Kernel interpolant of an arbitrary function:

$$\langle A(\mathbf{r}) \rangle = \int W(\mathbf{r} - \mathbf{r}', h) A(\mathbf{r}') d^3r'$$

If the function is only known at a set of discrete points, we approximate the integral as a sum, using the replacement:

$$d^3r' \mapsto \frac{m_j}{\rho_j}$$

$$\langle A_i \rangle = \sum_{j=1}^N \frac{m_j}{\rho_j} A_j W(\mathbf{r}_{ij}; h_i)$$



This leads to the SPH density estimate, for $A_i = \rho_i$

$$\rho_i = \sum_{j=1}^N m_j W(|\mathbf{r}_{ij}|, h_i)$$

→ This can be differentiated !

Kernel interpolants allow the construction of derivatives from a set of discrete tracer points

EXAMPLES FOR ESTIMATING THE VELOCITY DIVERGENCE

Smoothed estimate for the velocity field:

$$\langle \mathbf{v}_i \rangle = \sum_j \frac{m_j}{\rho_j} \mathbf{v}_j W(\mathbf{r}_i - \mathbf{r}_j)$$

Velocity divergence can now be readily estimated:

$$\nabla \cdot \mathbf{v} = \nabla \cdot \langle \mathbf{v}_i \rangle = \sum_j \frac{m_j}{\rho_j} \mathbf{v}_j \nabla_i W(\mathbf{r}_i - \mathbf{r}_j)$$

But alternative (and better) estimates are possible also:

Invoking the identity

$$\rho \nabla \cdot \mathbf{v} = \nabla \cdot (\rho \mathbf{v}) - \mathbf{v} \cdot \nabla \rho$$

one gets a "pair-wise" formula:

$$\rho_i (\nabla \cdot \mathbf{v})_i = \sum_j m_j (\mathbf{v}_j - \mathbf{v}_i) \nabla_i W(\mathbf{r}_i - \mathbf{r}_j)$$

What is smoothed particle hydrodynamics?

BASIC EQUATIONS OF SMOOTHED PARTICLE HYDRODYNAMICS

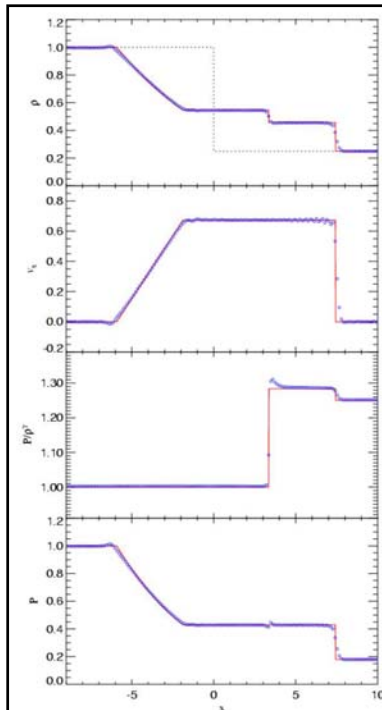
Each particle carries either the energy or the entropy per unit mass as independent variable

Density estimate $\rho_i = \sum_{j=1}^N m_j W(|\mathbf{r}_{ij}|, h_i) \rightarrow$ **Continuity equation automatically fulfilled.**

$\rightarrow P_i = (\gamma - 1)\rho_i u_i$

Euler equation $\frac{d\mathbf{v}_i}{dt} = - \sum_{j=1}^N m_j \left(\frac{P_i}{\rho_i^2} + \frac{P_j}{\rho_j^2} \right) \nabla_i \bar{W}_{ij}$
+ Π_{ij} Artificial viscosity

First law of thermodynamics $\frac{du_i}{dt} = \frac{1}{2} \sum_{j=1}^N m_j \left(\frac{P_i}{\rho_i^2} + \frac{P_j}{\rho_j^2} \right) \mathbf{v}_{ij} \cdot \nabla_i \bar{W}_{ij}$
+ Π_{ij}



An artificial viscosity needs to be introduced to capture shocks

SHOCK TUBE PROBLEM AND VISCOSITY

viscous force:

$$\left. \frac{d\mathbf{v}_i}{dt} \right|_{\text{visc}} = - \sum_{j=1}^N m_j \Pi_{ij} \nabla_i \bar{W}_{ij}$$

parameterization of the artificial viscosity:

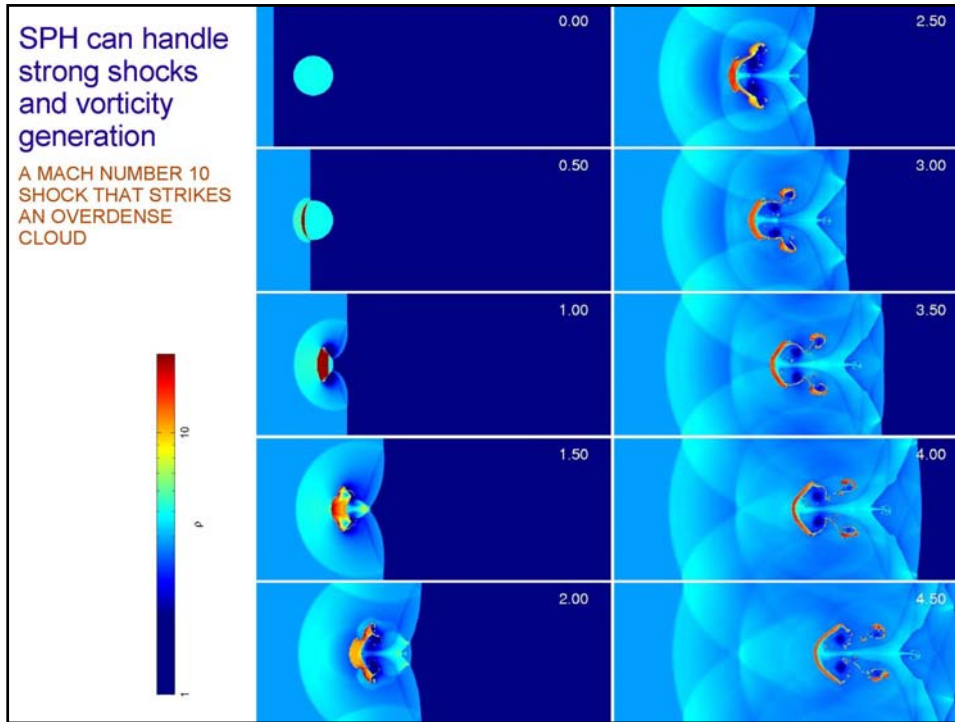
$$\Pi_{ij} = \begin{cases} -\frac{\alpha}{2} \frac{[c_i + c_j - 3w_{ij}]w_{ij}}{\rho_{ij}} & \text{if } \mathbf{v}_{ij} \cdot \mathbf{r}_{ij} < 0 \\ 0 & \text{otherwise} \end{cases}$$

$$v_{ij}^{\text{sig}} = c_i + c_j - 3w_{ij},$$

$$w_{ij} = \mathbf{v}_{ij} \cdot \mathbf{r}_{ij} / |\mathbf{r}_{ij}|$$

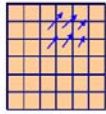

heat production rate:

$$\frac{du_i}{dt} = \frac{1}{2} \sum_{j=1}^N m_j \Pi_{ij} \mathbf{v}_{ij} \cdot \nabla_i \bar{W}_{ij}$$



There are principal differences between SPH and Eulerian schemes

SOME FUNDAMENTAL DIFFERENCE BETWEEN SPH AND MESH-HYDRODYNAMICS

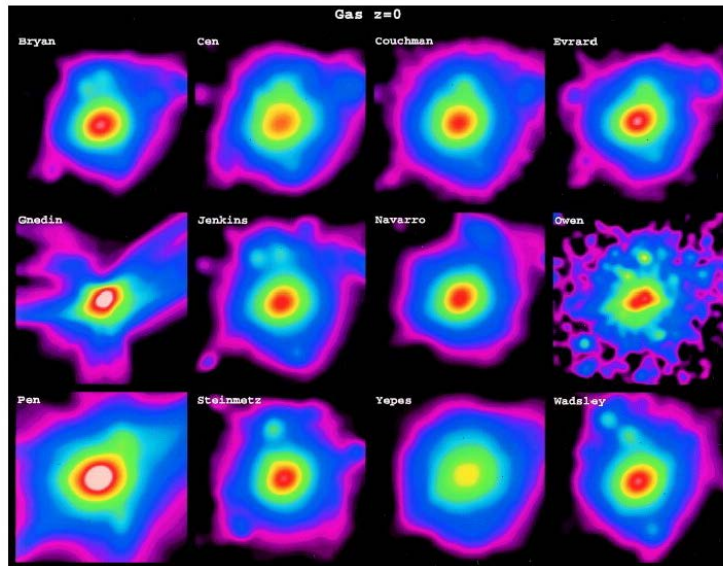
	Eulerian	Lagrangian	
	<p>sharp shocks, somewhat less sharp contact discontinuities (best schemes resolve fluid discontinuities in one cell)</p>	<p>shocks broadened over roughly 2-3 smoothing lengths (post-shock properties are correct though)</p>	
	<p>mixing happens implicitly at the cell level (but advection adds numerical diffusivity and may provide a source of spurious entropy)</p>	<p>mixing entirely suppressed at the particle-level (no spurious entropy production, but fluid instabilities may be suppressed)</p>	
	<p>no need for artificial viscosity (in Godunov schemes)</p>	<p>requires artificial viscosity</p>	
	<p>Truncation error not Galilean invariant (<i>"high Mach number problem"</i>)</p>	<p>Galilean invariant</p>	
	<p>self-gravity of the gas done on a mesh (but dark matter must still be represented by particles)</p>	<p>self-gravity of the gas naturally treated with the same accuracy as the dark matter, total energy conserved</p>	
	<p>no explicit conservation of total energy when self-gravity is included</p>		

Springel 2009

Different hydrodynamical simulation codes are broadly in agreement, albeit with substantial scatter and differences in detail

THE SANTA BARBARA CLUSTER COMPARISON PROJECT

Frenk, White & 23 co-authors (1999)

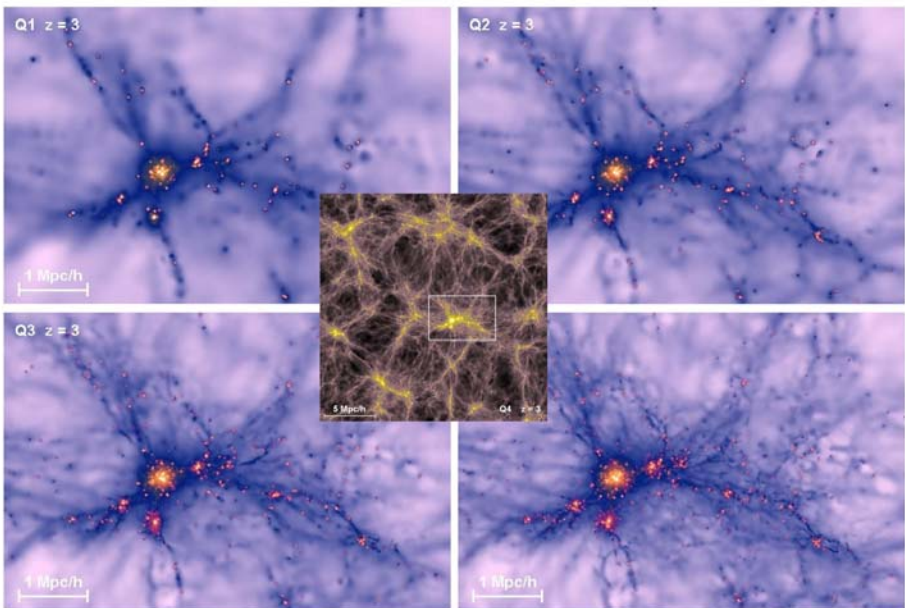


Nbody Simulations

a select number of results

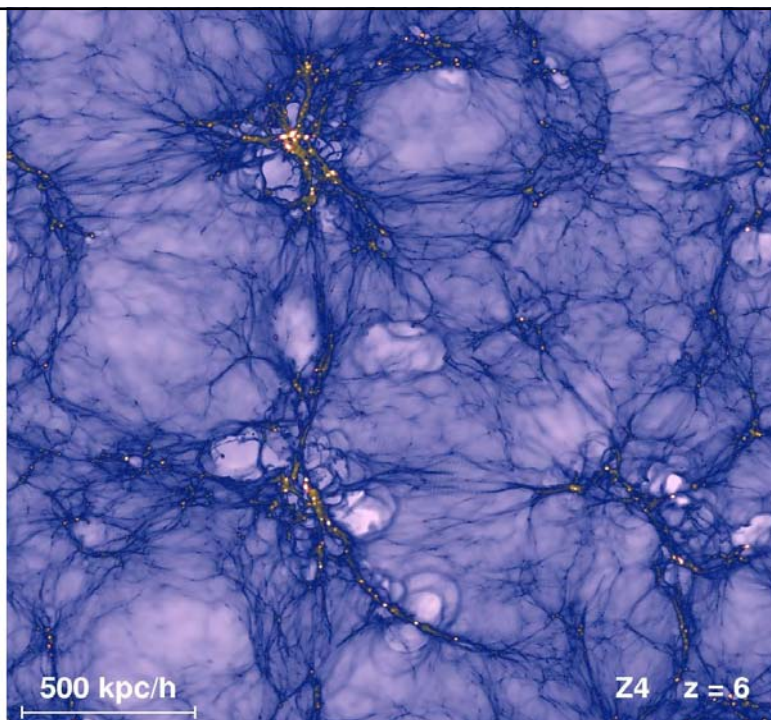
largely based on excellent Potsdam lectures on Nbody simulations (2006)
by V. Springel

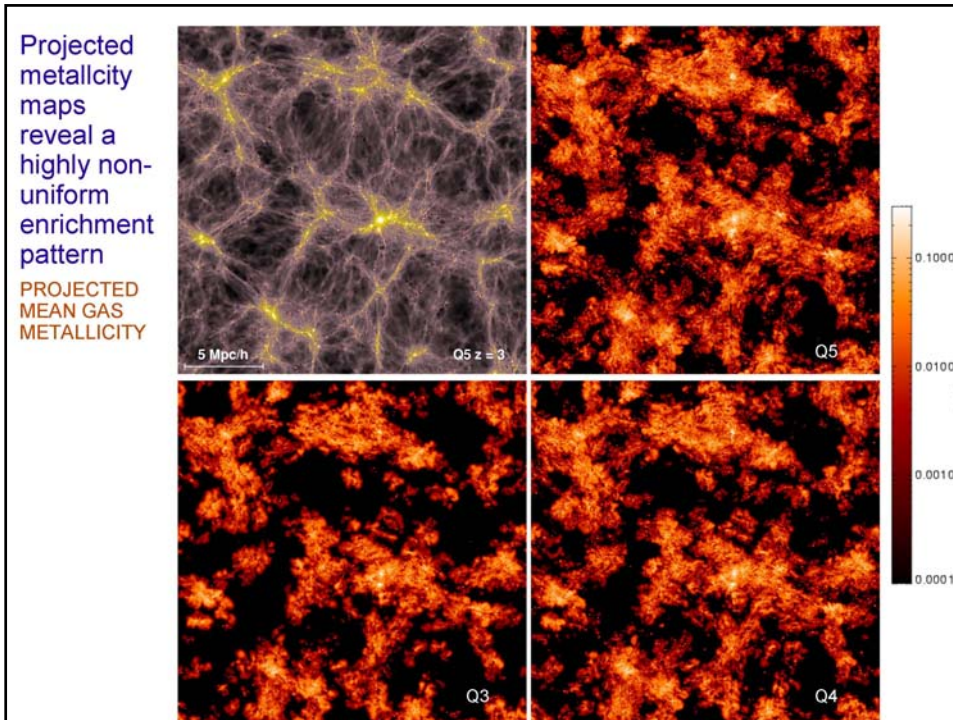
Higher mass resolution can resolve smaller galaxies

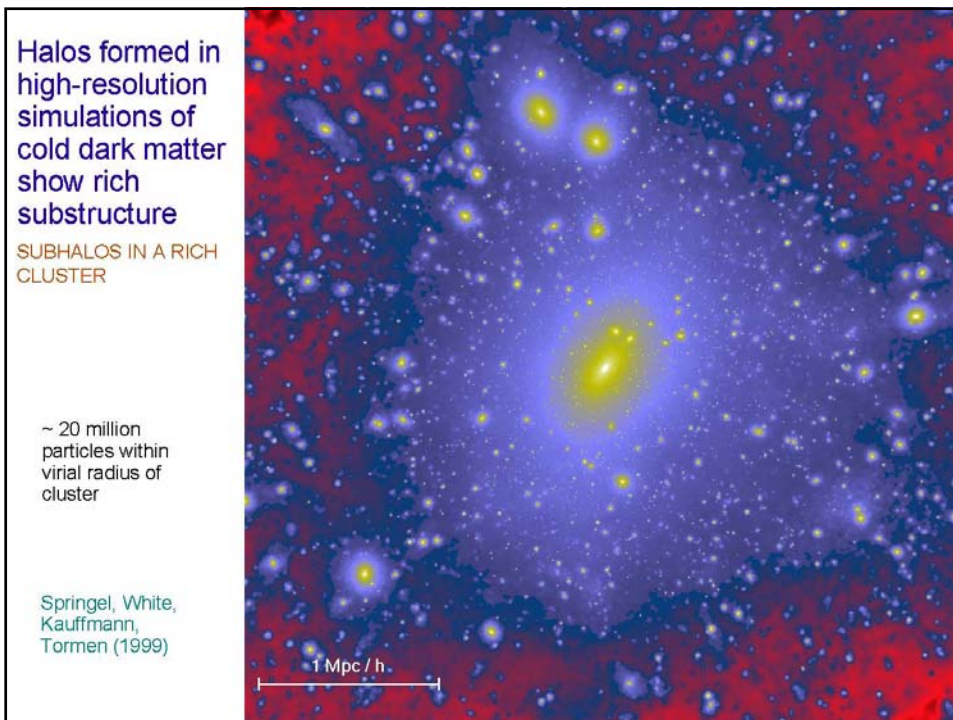
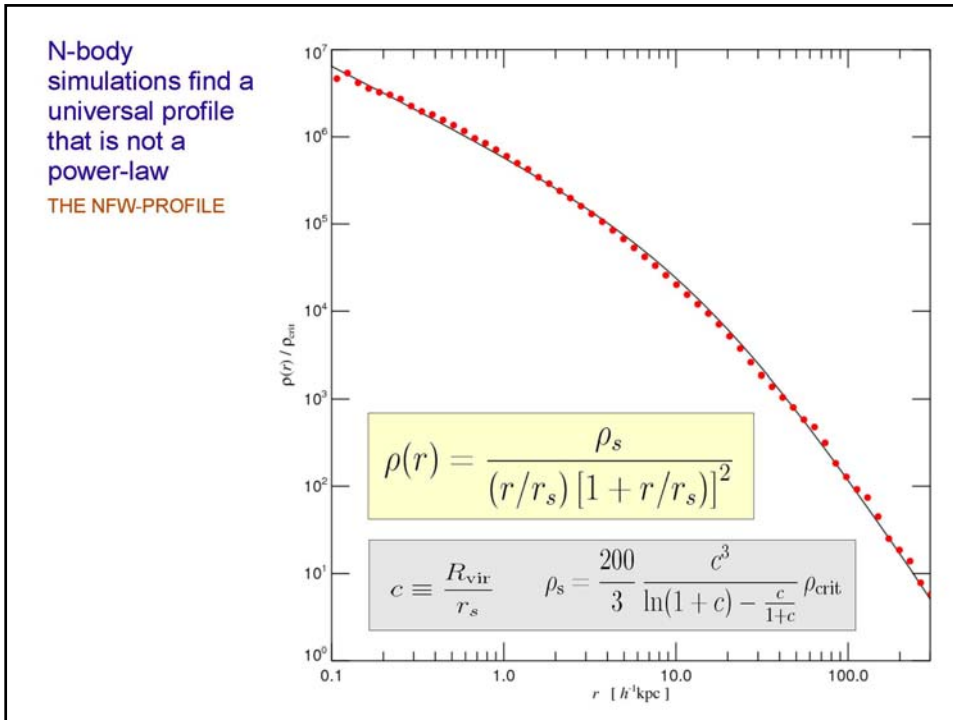


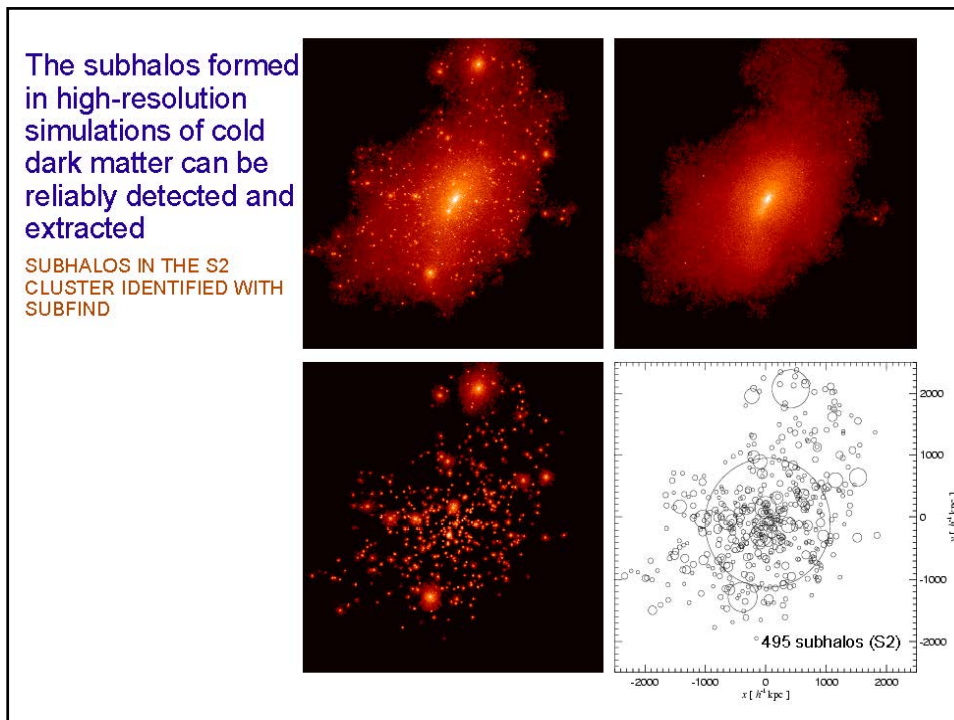
The "large-scale" structure seen at high redshift superficially resembles the morphology of structure seen at low redshift

GAS DISTRIBUTION SEEN IN A SMALL PERIODIC BOX AT REDSHIFT $z=6$

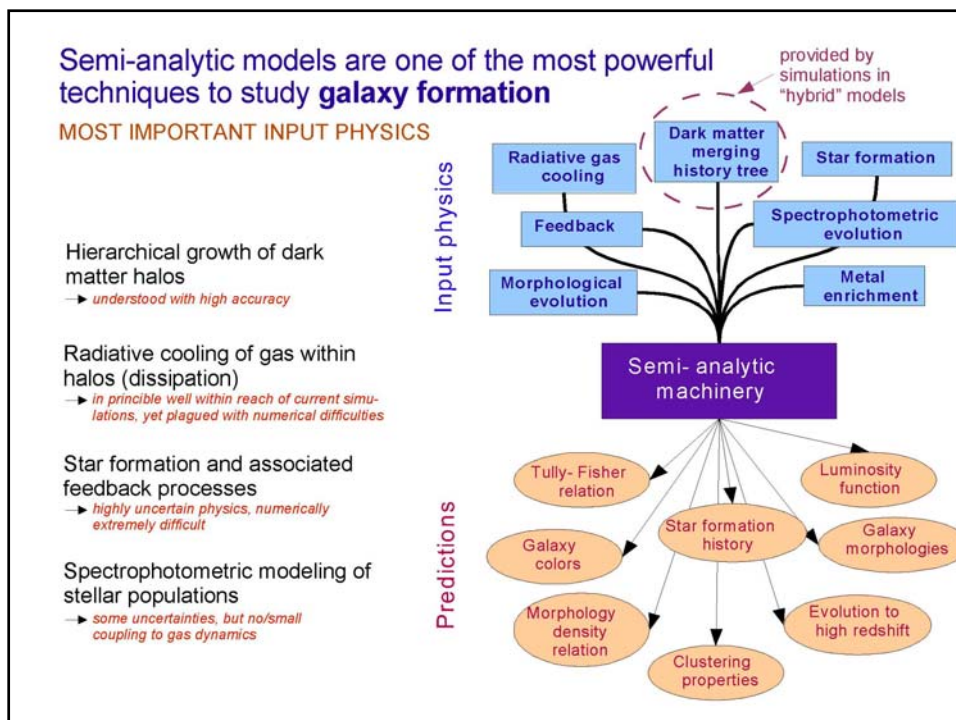
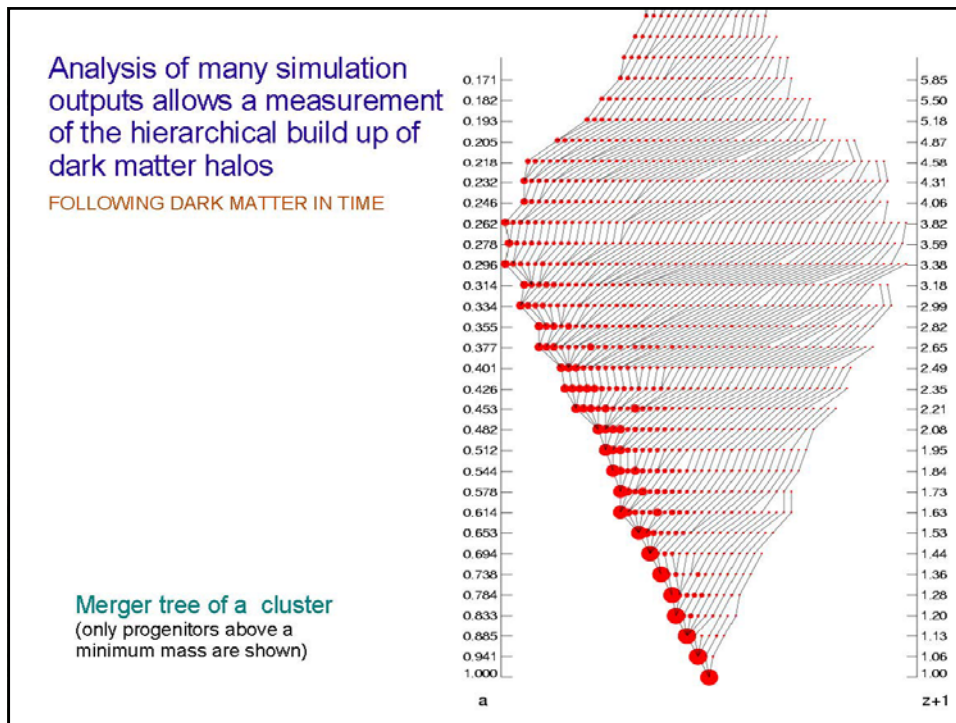


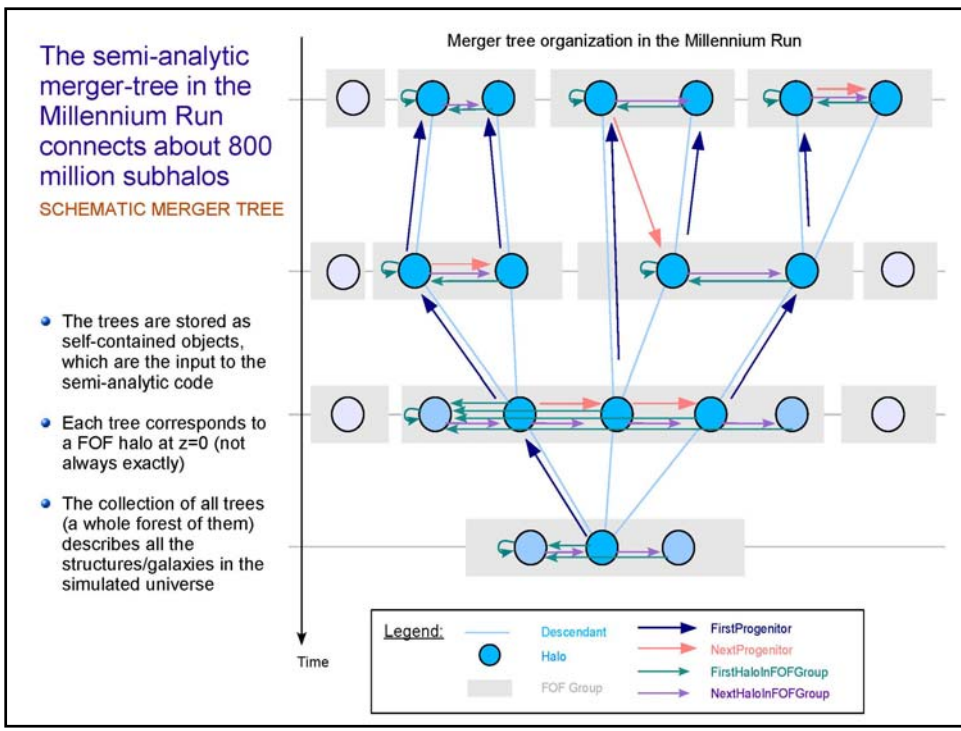
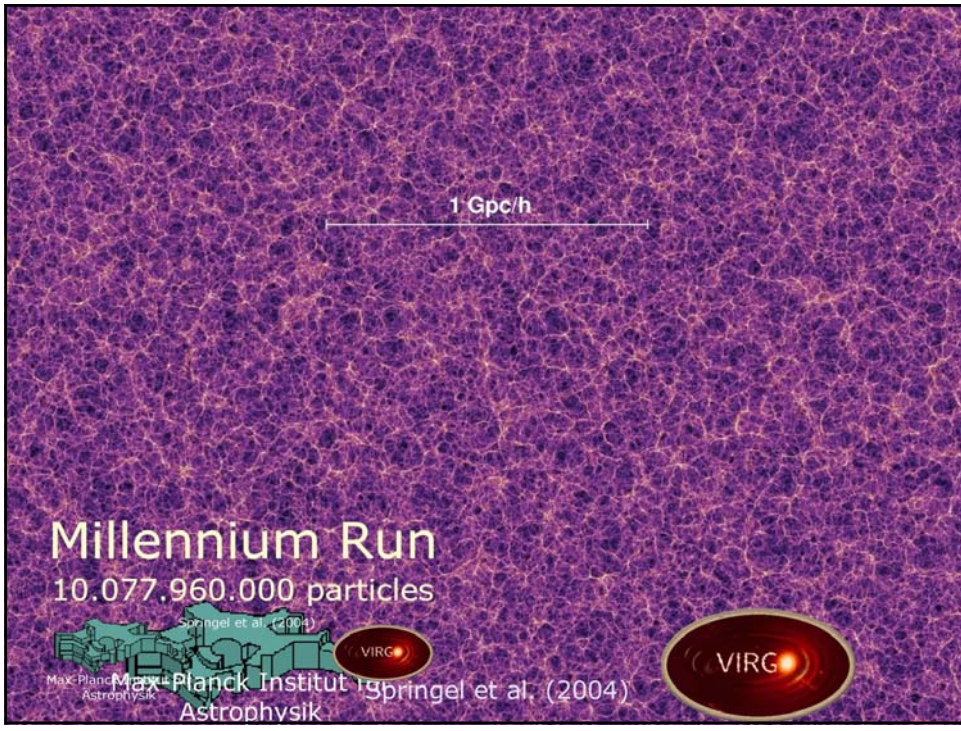






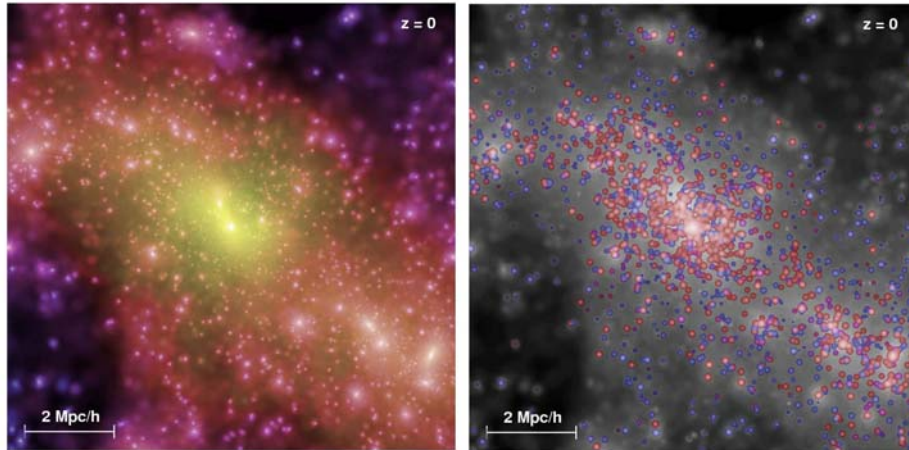
Semi-analytic Galaxy Formation & Subhalos





The merger tree in the Millennium simulation describes the orbits of all galaxies brighter than about $0.1 L_*$

DARK MATTER AND GALAXY DISTRIBUTION IN A CLUSTER OF GALAXIES



The distribution of dark matter on large scales

DARK MATTER DENSITY, COLOR-CODED BY DENSITY AND VELOCITY DISPERSION

